

MATERIALS SCIENCE

The β -relaxation in metallic glassesHai Bin Yu^{1,*}, Wei Hua Wang², Hai Yang Bai² and Konrad Samwer¹

ABSTRACT

Focusing on metallic glasses as model systems, we review the features and mechanisms of the β -relaxations, which are intrinsic and universal to supercooled liquids and glasses, and demonstrate their importance in understanding many crucial unresolved issues in glassy physics and materials science, including glass transition phenomena, mechanical properties, shear-banding dynamics and deformation mechanisms, diffusion and the breakdown of the Stokes–Einstein relation as well as crystallization and stability of glasses. We illustrate that it is an attractive prospect to incorporate these insights into the design of new glassy materials with extraordinary properties. We also outline important questions regarding the nature of β -relaxations and highlight some emerging research directions in this still-evolving field.

Keywords: metallic glass, β -relaxation, glass transition, shear transformation zone, shear band, diffusion, stability, ultrastable glass

INTRODUCTION AND HISTORICAL BACKGROUND

Glasses, by their general definition, are non-crystalline or amorphous solids that can be prepared via a variety of ways, such as by quenching from liquids. Glassy materials have been known and used by mankind for thousands of years, dating back to about 12 000 B.C. [1,2]. Although they are the oldest artificial materials, new discoveries and novel applications continue to appear [1]. Despite this, our understanding of glass is far from complete, and the nature of glass constitutes a long-standing puzzle in condensed matter physics [1–5].

Aside from their perplexing, disordered atomic arrangements, which are difficult to resolve and to relate to properties [6–10], glasses and glass-forming liquids are notorious for their extremely complex relaxation dynamics [1–5], ranging from picosecond-scale atomic vibrations to thousands of years, in some cases, for aging and densification [2]. These relaxation processes affect many properties of glassy materials. On a typical, experimentally observable isothermal relaxation spectrum (as schematically shown in Fig. 1) [2], glass-forming materials show α -relaxation at low frequency ($\sim 10^{-2}$ Hz in Fig. 1), β -relaxation and faster processes at higher frequency ($\sim 10^6$ Hz), and the Boson peak at even higher frequency ($\sim 10^{12}$ Hz). The α -relaxation is

the main relaxation mode, and is directly related to viscous flow and the glass transition, which has been regarded as the central feature of glassy physics [1–5]. However, because the α -relaxation is frozen below the glass transition temperature T_g , the β -relaxation becomes the most important relaxation process in the glassy state. Significantly, it has recently been shown that the β -relaxation has considerable potential for explaining many unresolved issues in glassy physics and materials science [5,11–13]. The aim of this paper is to provide a state-of-the-art review on β -relaxation in a relatively new kind of glassy materials, the metallic glasses (MGs), paying special attention to the implications for our understanding of glass transition phenomena, mechanical properties, shear-banding dynamics and deformation mechanisms, diffusion and the breakdown of the Stokes–Einstein relation, as well as crystallization and stability of glasses. MGs are different from other glasses because of their simple atomic structures, which means that they are free of motions from internal degrees of freedom [10] (e.g. side chains in polymers and functional groups in molecular glasses); they also have widely tunable compositions. These features have made MGs important model materials for studying the above topics (as well as many others) in glassy physics [11,14].

¹Physikalisches Institut, Universität Göttingen, D-37077 Göttingen, Germany; and ²Institute of Physics, Chinese Academy of Sciences, Beijing 100190, China

*Corresponding author. E-mail: hyu1@gwdg.de

Received 14 November 2013;
Revised 3 January 2014; Accepted 6 January 2014

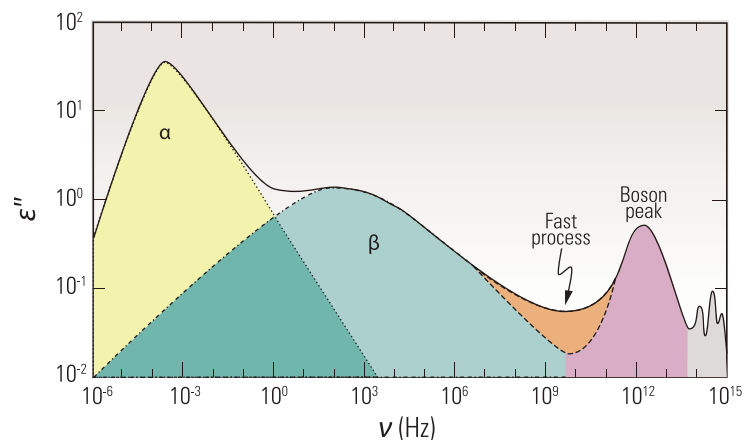


Figure 1. Schematic dielectric spectrum of relaxation dynamics of glass-forming liquids (Courtesy of P. Lunkenheimer, University of Augsburg, Germany).

Historically, the β -relaxation was first known in polymer glasses, as a secondary relaxation in internal friction measurements, occurring at temperatures far below T_g and having important connections with mechanical properties [15–18]. The terminology ‘ β -relaxation’ was simply used because it comes after the α -relaxation in a relaxation spectrum. Because of the chain-like structures of polymers, β -relaxation was initially assumed to originate from rotations of the side chains or functional groups of polymers. However, this view was changed in the 1960s and 1970s when Johari and Goldstein discovered β -relaxations in a series of rigid polymers and molecular glasses, which did not have side chains or internal degrees of freedom [19–22]. These findings implied that some β -relaxations must not involve intramolecular motions but instead certain motions of the entire molecule as a whole. In 2004, Ngai and Paluch [23] classified the β -relaxations in different glass formers based on their dynamic properties; they named the type of β -relaxations that do not involve intramolecular motion as ‘Johari–Goldstein β -relaxations’ to distinguish them from other β -relaxations (which do involve intramolecular motion) and also to honor the important discovery of Johari and Goldstein. In fact, in some molecular and polymer glasses, there are multiple secondary relaxations, but some of these arise from intramolecular degrees of freedom (and thus lack universal significance). Only *intermolecular* secondary relaxations (or Johari–Goldstein β -relaxations) are considered of fundamental importance [23].

Contemporary to the discovery of Johari and Goldstein β -relaxations, MGs were created by rapid quenching of metallic melts [24]. Combining metallic bonding and disordered structures and free of traditional crystalline defects (e.g. dislocations and grain boundaries), MGs, besides their fascinating

properties and potential to revolutionize the fields of materials science and engineering [25,26], soon became a kind of model material in glassy physics. Since the 1980s, Chen and co-workers made internal friction measurements on some typical Pd and La MGs [27–30], and they observed the signatures of β -relaxations in MGs. However, limited by the low glass-forming ability and/or the low thermal stability of the MGs available at that time, β -relaxations had not been unambiguously determined. Since the 1990s, the development of bulk metallic glasses (BMGs) [31–34] with excellent glass-forming ability and thermal stability opened a new avenue to study of β -relaxations. Notably, clear correlations found between β -relaxations and other processes and properties in BMGs make study of β -relaxations in MGs a promising route to understand many fundamental issues in glassy physics and materials science [11].

MEASUREMENTS OF β -RELAXATIONS IN MGs

In non-MGs, dielectric spectroscopy is a standard tool to study the relaxation behavior, taking advantage of its wide frequency range (e.g. 10^{-2} – 10^{12} Hz) and high sensitivity [2]. Since MGs are good conductors, the dielectric method is not feasible. Other methods such as dynamical mechanical analysis (DMA), differential scanning calorimetry (DSC), and, recently, scanning tunneling microscopy (STM) are employed in an effort to study the relaxation behavior of MGs. Among them, DMA is commonly used because of its wide applicability and high sensitivity in detecting atomic rearrangements associated with defects in solids.

Dynamical mechanical analysis

DMA [also known as dynamical mechanical spectroscopy (DMS)] is a thermal analysis technique that measures properties of materials as they are deformed under a periodic stress. Specifically, in a DMA measurement, a sinusoidal stress (or strain) is applied to the sample and the resultant sinusoidal strain (or stress) is measured. If the material being evaluated is purely elastic, the phase difference δ between the stress and strain sine waves is 0° (i.e. they are in phase). If the material is purely viscous, δ is 90° . However, most real materials are viscoelastic and exhibit a phase difference somewhere between those two extremes. From this phase difference δ , together with the amplitudes of the stress and strain waves, a variety of fundamental material parameters can be determined, including the storage

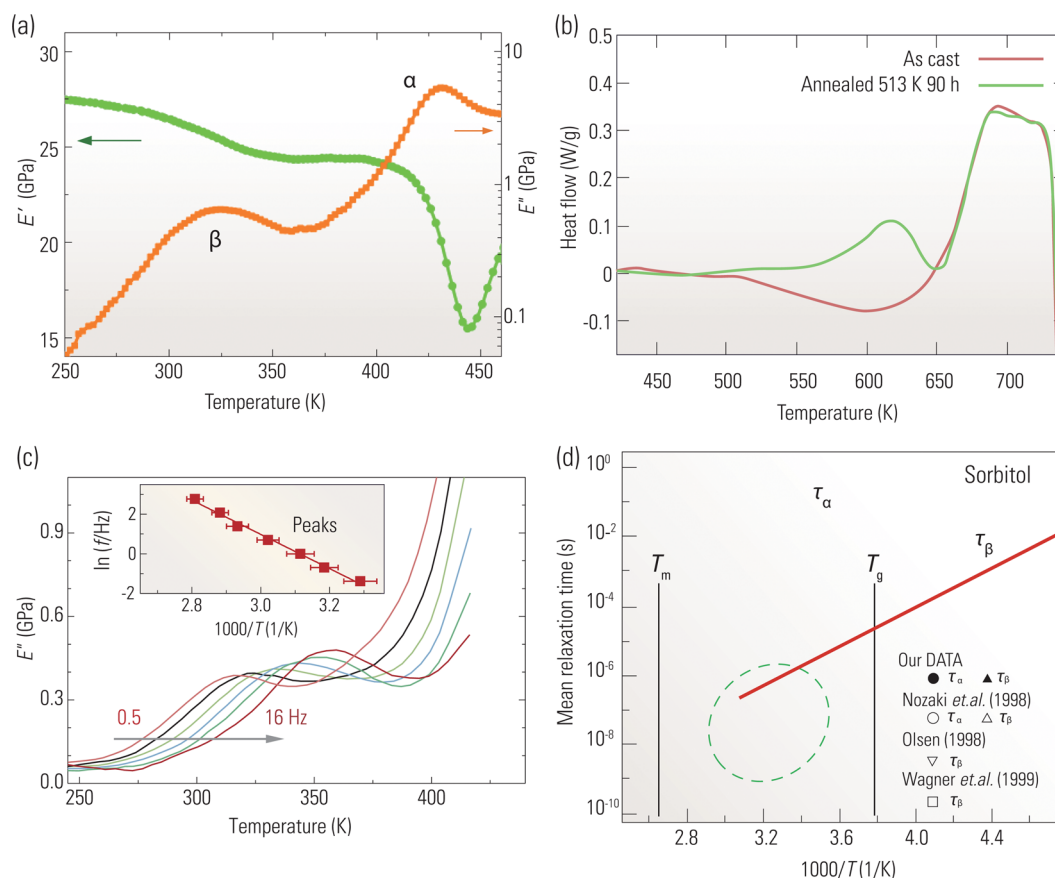


Figure 2. Typical features of β -relaxations. **(a)** The temperature-dependent E' (left axis) and E'' (right axis), measured by DMA at a test frequency of 1 Hz for a $\text{La}_{68.5}\text{Ni}_{16}\text{Al}_{14}\text{Co}_{1.5}$ MG [11,35]. **(b)** DSC curves of an as-cast and an annealed $\text{Zr}_{65}\text{Cu}_{27.5}\text{Al}_{7.5}$ MG [55]. **(c)** Temperature-dependent E'' of a $\text{La}_{68.5}\text{Ni}_{16}\text{Al}_{14}\text{Co}_{1.5}$ MG [11,35] at different frequencies (from left to right: 0.5, 1, 2, 4, 8, and 16 Hz); the inset is the Arrhenius plot of the peak temperature and frequency corresponding to the β -relaxation (Copyright 2011 American Physics Society). **(d)** Relaxation times for α and β -relaxations of sorbitol in the merging region, adapted from [73] (Copyright 2002 American Physics Society).

modulus E' , loss modulus E'' , loss tangent $\tan(\delta)$, and frequency-dependent transition temperatures.

Fig. 2a presents a typical DMA measurement on a $\text{La}_{68.5}\text{Ni}_{16}\text{Al}_{14}\text{Co}_{1.5}$ MG [11,35], which shows the temperature dependence of E' and E'' , at a single test frequency $f = 1$ Hz. The E'' curve shows two distinct peaks: the one at higher temperature (440 K) corresponds to the α -relaxation while that at lower temperature (330 K) is the β -relaxation. Some common features of the β -relaxation are discussed in the section entitled 'TYPICAL FEATURES OF β -RELAXATIONS'. Up until now, DMA has been used to study β -relaxations in various MGs [36–50].

Annealing and calorimetry

Without varying the frequency, the identification of β -relaxations is not as straightforward. Despite this, there have been substantial studies of β -relaxations

using DSC measurements, usually involving careful annealing treatments [51–54]. Fig. 2b compares the DSC curves for as-cast and annealed (at 513 K, 90 h) $\text{Zr}_{65}\text{Cu}_{27.5}\text{Al}_{7.5}$ MGs [55]. A pronounced exothermic peak develops below T_g in the annealed sample. This exothermic process was regarded as an indirect signature of the β -relaxation, as it coincides with the drop in storage modulus and increase in loss modulus from the DMA measurements [51–54]. The characteristic temperature of the exothermic relaxation peak increases with increasing heating rate; the activation energy determined from this dependence is usually of similar order to that measured by DMA. This approach has been used in studies of amorphous pharmaceuticals and glassy polymers, as well as MGs [51–54]. However, it should be noted that annealing at relatively high temperature could activate portions of the high-energy states in the spectrum of structural relaxations, and thus only

results from lower temperature annealing are relevant to β -relaxations.

Hyperquenching–annealing–calorimetry

Hu and Yue introduced another approach to detect the β -relaxation processes by DSC [13, 56–61]. Their aim was to freeze the liquid at a high-temperature configuration and to probe the calorimetric enthalpy relaxation by DSC after annealing treatments below T_g . All potential energy states in the temperature range could be observed in a real-time window during the following enthalpy-recovery procedures. In this way, Yue and co-workers made initial studies on the β -relaxation in oxide glasses [56,57], and Hu *et al.* reported the characteristics of the β -relaxation in some oxide glasses and MGs [13,58–63]. Some abnormal behavior was also observed [60–62].

Inferences from the observation of surface dynamics by STM

Recently, Ashtekar *et al.* [64,65] successfully visualized the surface dynamics of some MGs by STM. They found that the rearrangements of surface clusters occur almost exclusively by two-state hopping, and that the dynamics are both spatially and temporally heterogeneous. They argue that their observed surface dynamics are a consequence of the β -relaxations in MGs, because the relaxation times for α -relaxation are much longer than their experimental timescale, and, at temperatures far below T_g , the mobility of atoms can only be initiated by β -relaxations.

It should be noted that study of the surface glassy dynamics by STM is a relatively new approach and the exact nature of what it measures is still not fully established. Nevertheless, because of the good conductivity of MGs, the application of STM in studying surface dynamics is anticipated to provide deep insights into the dynamics of glassy materials.

TYPICAL FEATURES OF β -RELAXATIONS

Before discussing the importance of β -relaxations in MGs, we briefly address the typical features and possible mechanisms of β -relaxations. Because the temperature and frequency ranges of mechanical spectroscopies are limited, and many MG-forming liquids also crystallize, many properties of β -relaxations in MGs are still not explored; therefore, some general features inferred from or-

ganic glass-forming materials are included here and discussed.

Wide and symmetric distribution of relaxation times

As can be seen from Fig. 2a, the E'' peak corresponding to the β -relaxation measured by DMA spans a wide temperature range, from below 250 to above 350 K in the case of $\text{La}_{68.5}\text{Ni}_{16}\text{Al}_{14}\text{Co}_{1.5}$ MG. Such a wide and symmetric peak indicates that the β -relaxation has a wide distribution of relaxation times. This feature is more obviously seen in the frequency domain for organic glass-forming materials, as probed by dielectric spectroscopy [2–5,66–68]. Detailed study of the shapes of the dielectric spectra of organic glass-forming materials revealed that the β -relaxation can be described in terms of a Gaussian distribution of Debye-type processes, which correspond to local intermolecular excitations (reorientation or diffusion) [66–69]. Recently, Jiao *et al.* introduced a stress relaxation approach to characterize the distribution and evolution of energy barriers around the temperature range of the β -relaxation in a Pd-based MG [70]. They suggested that the distribution of energy barriers becomes wider with increasing temperature. However, it should be noted that theoretical and experimental work on non-MGs demonstrates that the distribution of energy barriers in non-MGs becomes narrower with increasing temperature [66–69].

Low amplitude and increases with temperature

In the glassy state, the amplitude or strength of the β -relaxation is usually low compared to that of the α -relaxation and it is weakly temperature dependent. For MGs, the E'' value for the β peak is about 1/10 of that of the α peak [11]. However, in many organic systems, the strength of the β -relaxation increases rapidly above T_g , meaning that it has a similar temperature dependence to that of other thermodynamic properties of the system, including entropy, enthalpy, and volume [5,12,13]. Such behavior has been considered as evidence that the β -relaxation is connected to the glass transition [5,12,13]. Contrary to the behavior of the β -relaxation, the strength of the α -relaxation decreases with increasing temperature [68,69]. It is noted that the β -relaxation in MG-forming liquids has not been explored at temperatures higher than T_g , partly because of the intervention of rapid crystallization at intermediate supercooling temperatures.

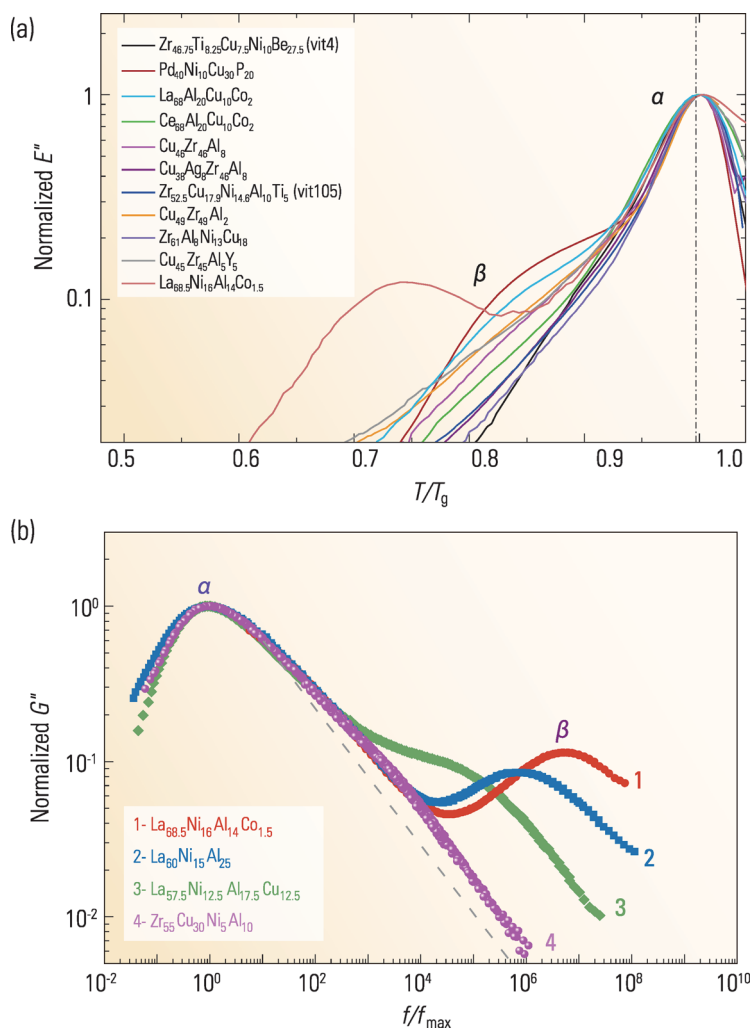


Figure 3. Comparison of the behavior of β -relaxations (measured by DMA) between typical MGs in (a) normalized temperature frame (Copyright 2011 American Physics Society) and (b) normalized frequency frame [46] (Copyright 2011 American Institute of Physics).

Arrhenius-type temperature dependence of the relaxation time in the glassy state

Fig. 2c displays the dynamical features of the β peaks. The peak temperature of E'' , T_p , increases markedly with f , during isochronous measurements. The inset of Fig. 2c shows the f -dependent peak temperature T_p from Fig. 2c. These data can be fitted by an Arrhenius equation:

$$f = f_{\infty} \exp(-E_{\beta}/RT_p), \quad (1)$$

where f_{∞} is the prefactor and E_{β} the activation energy of the β -relaxation. Arrhenius behavior is a general property of β -relaxation in glassy states, and E_{β} is an important parameter for obtaining quantitative insights. On the other hand, many studies in non-MG-forming liquids have revealed that the Arrhenius-type temperature dependence changes

to a stronger one above T_g , in accordance with the rapid increase in strength of the β -relaxation [71–73]. The exact relationship between f and T_p at $T > T_g$ has not been established.

Merging with α -relaxation at high temperatures

As shown in Fig. 2d for an organic glass-forming liquid, sorbitol [73], the relaxation times of α - and β -relaxations become closer with increasing temperature in the supercooled liquid, and, finally, at a temperature called the crossover temperature T_c , they merge into a single relaxation process. As the temperature-dependent relaxation time of the β -relaxation changes across T_g , the issue of how the β -relaxation merges with the α -relaxation is not very clear. T_c has been regarded as crucial to understanding the nature of glass and the physics of the glass transition, because many exceptional phenomena appear there [74–79]. Moreover, T_c lies close to characteristic temperatures that are identified in several different theories and models, and these topics are currently being actively studied in the field of glassy physics. In MGs, the merging of α - and β -relaxations has been inferred [80], but there are still no direct experimental measurements in supercooled liquids.

DIFFERENT BEHAVIORS OF β -RELAXATIONS: PEAKS OR EXCESS WINGS

Glasses and glass-forming liquids show different β -relaxation behaviors. In some supercooled liquids and glasses, β -relaxations exhibit distinct peaks or humps in the dielectric or mechanical loss spectra, while in other systems β -relaxations appear to be absent; instead, an excess contribution to the tail of the α -relaxation is observed. Fig. 3 illustrates this point in several typical MGs [11,35,46]. This so-called ‘excess wing’ has been observed in many systems without a well-resolved β -relaxation peak. Historically, excess wings and β -relaxations were considered to be two different phenomena, and the corresponding materials were defined as type A and B glass formers, respectively [2]. Now, after intensive studies in different glass-forming materials, it is commonly recognized that they are similar in nature and the excess wing is due to an underlying β -relaxation. However, different views on the nature of the β -relaxations still persist.

It is important to clarify the dominant factors that govern the behavior of β -relaxations because β -relaxations affect many material properties.

For example, polymers and MGs with pronounced β -relaxations at relatively low temperatures usually exhibit good ductility and are favored for mechanical applications, while, in the pharmaceuticals industry, β -relaxations are sometimes undesired and should be suppressed, because they cause the devitrification and destabilization of glassy medicines.

In the following section, we review different β -relaxation behaviors in MGs (from peaks to excess wings). Special emphasis is placed on the factors that influence this behavior, including composition (chemical), aging, and thermal history effects.

Chemical influence on the behavior of β -relaxations in MGs

As can be seen from Fig. 3, chemical composition affects the behavior of β -relaxations in MGs. Recently, Yu *et al.* [81] systematically studied the chemical (composition) effects on β -relaxations in several typical MG systems, and formulated a general rule about the behavior of β -relaxations in MGs from the perspective of enthalpy of mixing; namely, pronounced β -relaxations are associated with systems where all the atomic pairs have large similar negative values of enthalpy of mixing, while positive values, or large fluctuations in the values, of enthalpy of mixing suppress β -relaxations. They suggested that the underlying physical picture is that strong and comparable interactions among all the constituent atoms maintain string-like atomic configurations, which enable excitation of β -events; these glasses can be thought of as ‘molecular metallic glasses’ [81].

For example, the left panel of Fig. 4a–c [81] shows the temperature T -dependent loss modulus E'' of three prototypical MG systems (La–Ni/Cu–Al, Pd–Ni/Cu–P, and Cu–Zr–Al) in a normalized frame, where T and E'' are scaled by T_g and $E''(T = T_g)$, respectively. From Fig. 4a–c, the following features can be directly observed.

- (i) In the $\text{La}_{70}(\text{Cu}_x\text{Ni}_{1-x})_{15}\text{Al}_{15}$ MGs, Fig. 4a, Cu suppresses β -relaxations (i.e. makes them less pronounced), while Ni promotes them.
- (ii) Cu promotes β -relaxations in the $\text{Pd}_{40}(\text{Cu}_x\text{Ni}_{1-x})_{40}\text{P}_{20}$ system, Fig. 4b, while Ni suppresses them.
- (iii) Microalloying of Al in CuZr MGs drastically suppresses the shoulder and an excess wing shows up instead (see Fig. 4c).

In general, these features demonstrate strong yet complicated (system-specific) chemical effects on the β -relaxation in MGs. Especially, comparing (i) and (ii) indicates that the effect of Ni/Cu on the β -relaxation is not solely determined by their atomic properties, but must also depend on their specific

chemical environments and interactions with other constituent atoms.

To understand these chemical effects, Yu *et al.* considered the enthalpies of mixing for these MGs [81]. The right panel of Fig. 4a–c displays the values of enthalpy of mixing $\Delta H_{AB}^{\text{mix}}$ for different atomic pairs in three prototypical MG systems. These values are obtained from Miedema’s model for binary alloys, which is a semi-quantitative theory based on the thermodynamics of matter and energy band theory. A closer examination of the $\Delta H_{AB}^{\text{mix}}$ values for these different atomic pairs reveals a pattern. In systems with pronounced β -relaxations, all the atomic pairs have similarly large negative values of $\Delta H_{AB}^{\text{mix}}$, while systems with positive enthalpies of mixing or large differences in the enthalpies of mixing of the various components are associated with less pronounced β -relaxations or excess wings. For instance, in the La–Ni–Al system, with pronounced β -relaxations, the $\Delta H_{AB}^{\text{mix}}$ values for La–Ni, La–Al, and Ni–Al atomic pairs are -28 , -37 , and -22 kJ/mol, respectively, while in the La–Cu–Al system with less pronounced β -relaxations, $\Delta H_{AB}^{\text{mix}}$ for Al–Cu is -1 kJ/mol, much smaller in magnitude than those for the other two atomic pairs (-21 and -37 kJ/mol for La–Cu and La–Al pairs, respectively), and thus there are large differences in enthalpy of mixing between different atomic pairs. This finding is also applicable to the Pd–Cu/Ni–P and Zr–Cu–Al systems, as shown in Fig. 4b and c, and to 12 other systems with a variety of compositions [81], as summarized in Table 1. Both the magnitudes and fluctuations of chemical interactions between constituent atoms influence the β -relaxation behavior in MGs. Specifically, strong and comparable interactions among all the constituent atoms, which might be viewed as local formation of a ‘molecule’, are favorable for pronounced β -relaxations; the lack of these interactions generally leads to excess wings.

In some MG systems (e.g. La–Ni/Cu–Al and Pd–Ni/Cu–P), the above ‘chemical fluctuation arguments’ can be coarse-grained by a ‘mean-field-like’ approach by defining a mean chemical affinity:

$$\Delta H^{\text{chem}} = 4 \sum_{A \neq B} \Delta H_{AB}^{\text{mix}} c_A c_B \quad (2)$$

(where c_A and c_B are the molar percentages of elements A and B, respectively). In the $\text{La}_{70}(\text{Cu}_x\text{Ni}_{1-x})_{15}\text{Al}_{15}$ and $\text{Pd}_{40}(\text{Cu}_x\text{Ni}_{1-x})_{40}\text{P}_{20}$ MGs, Yu *et al.* [81] found that the dependence of ΔH^{chem} against x is indeed correlated with the composition-dependent β -relaxation behavior; larger negative values of ΔH^{chem} yield more pronounced β -relaxations, see Fig. 5a. This correlation, although it does not really clarify the underlying

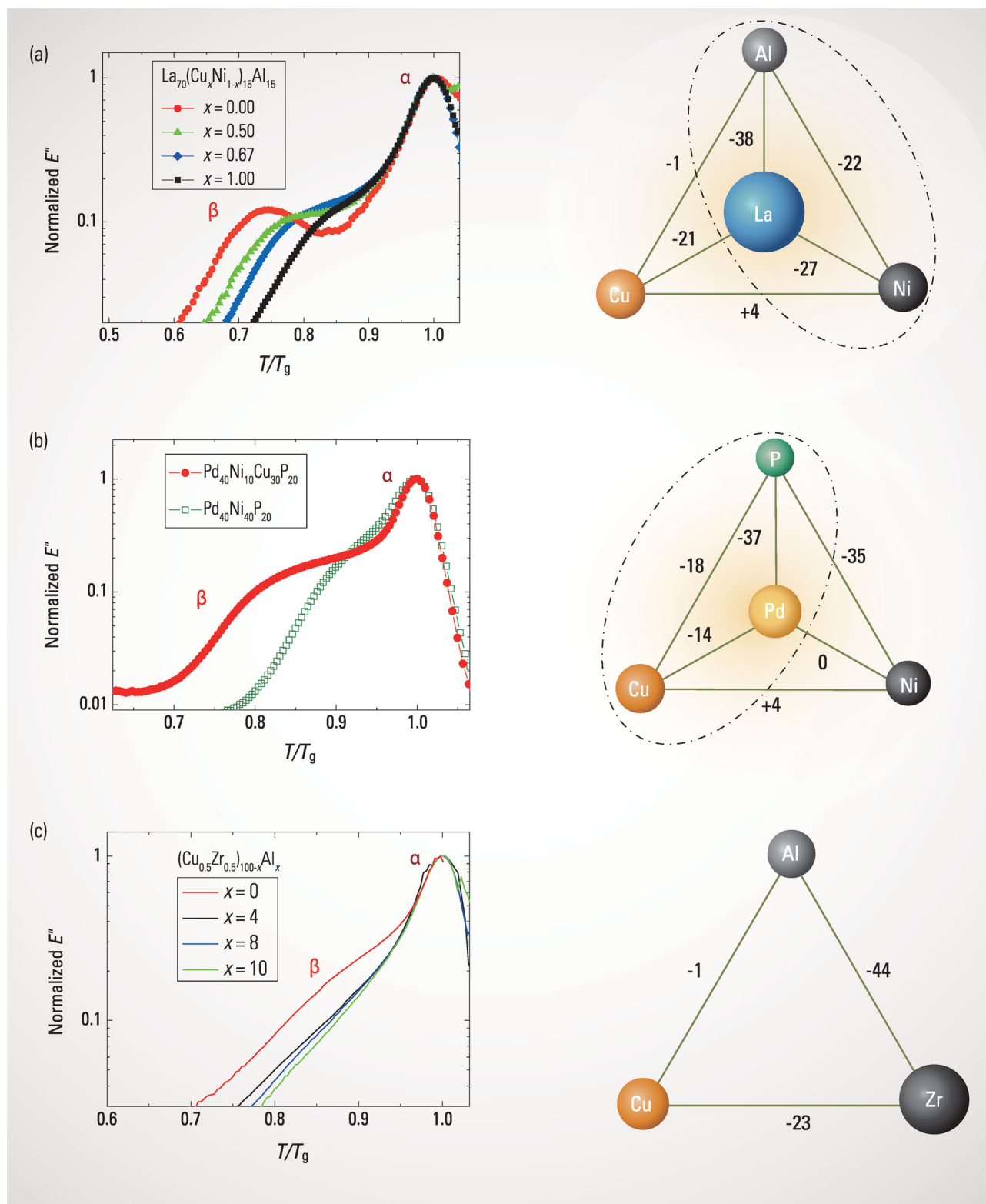
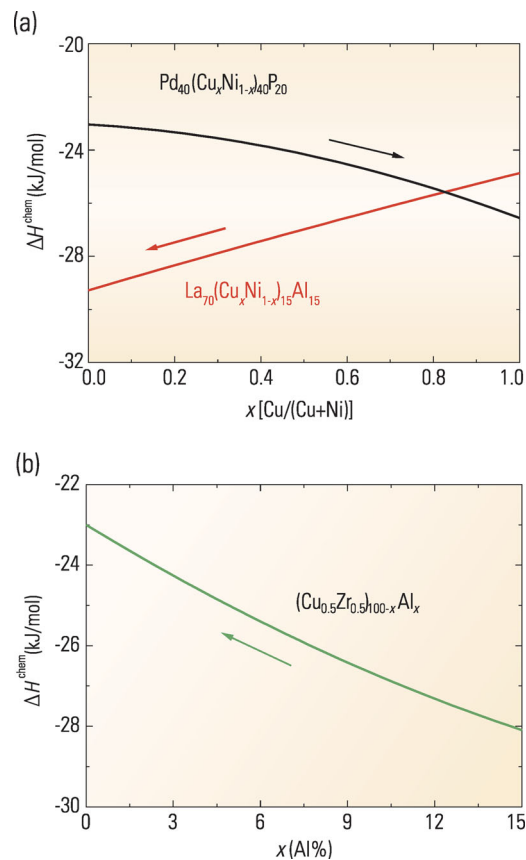


Figure 4. (Left panel) Chemical effects on β -relaxations in typical (a) La-based, (b) Pd-based, and (c) CuZr-based MGs. (Right panel) Enthalpy of mixing of corresponding MGs. The dash-dotted ellipses indicate compositions with pronounced β -relaxations [81] (Copyright 2013 Nature Publishing Group).

Table 1. The β -relaxations in different MG systems and the enthalpies of mixing between their constituent atoms.

#	MG system	β -relaxation (DMA)	ΔH_{AB} (kJ/mol)
1	La-Ni-Al	Peaks	$\Delta H_{La-Ni} = -27$
			$\Delta H_{La-Al} = -38$
			$\Delta H_{Ni-Al} = -22$
2	La-Cu-Al	Shoulders	$\Delta H_{La-Cu} = -21$
			$\Delta H_{La-Al} = -38$
			$\Delta H_{Cu-Al} = -1$
3	La-Co-Al	Peaks	$\Delta H_{La-Co} = -17$
			$\Delta H_{La-Al} = -38$
			$\Delta H_{Co-Al} = -19$
4	Sm-Co-Al	Peaks	$\Delta H_{Sm-Co} = -22$
			$\Delta H_{Sm-Al} = -38$
			$\Delta H_{Co-Al} = -19$
5	Ce-Cu-Al	Excess wings	$\Delta H_{Ce-Cu} = -21$
			$\Delta H_{Ce-Al} = -38$
			$\Delta H_{Cu-Al} = -1$
6	Ce-Ni-Al	Peaks/humps	$\Delta H_{Ce-Ni} = -28$
			$\Delta H_{Ce-Al} = -38$
			$\Delta H_{Ni-Al} = -22$
7	Pd-Cu-P	Humps	$\Delta H_{Pd-Cu} = -14$
			$\Delta H_{Pd-P} = -37$
			$\Delta H_{Cu-P} = -18$
8	Pd-Ni-P	Shoulders	$\Delta H_{Pd-Ni} = 0$
			$\Delta H_{Pd-P} = -37$
			$\Delta H_{Ni-P} = -35$
9	Zr-Cu-Al	Excess wings	$\Delta H_{Zr-Cu} = -23$
			$\Delta H_{Zr-Al} = -44$
			$\Delta H_{Cu-Al} = -1$
10	Cu-Zr-Ag	Excess wings	$\Delta H_{Cu-Zr} = -23$
			$\Delta H_{Cu-Ag} = 2$
			$\Delta H_{Zr-Ag} = -20$
11	Cu-Zr-Be	Excess wings	$\Delta H_{Cu-Zr} = -23$
			$\Delta H_{Cu-Be} = 0$
			$\Delta H_{Zr-Be} = -43$
12	Cu-Ti-Be	Excess wings	$\Delta H_{Cu-Ti} = -9$
			$\Delta H_{Cu-Be} = 0$
			$\Delta H_{Ti-Be} = -30$
13	Pd-Cu-Si	Humps	$\Delta H_{Pd-Cu} = -14$
			$\Delta H_{Pd-Si} = -55$
			$\Delta H_{Cu-Si} = -19$
14	Zr-Ni-Al	Humps/shoulders	$\Delta H_{Zr-Ni} = -49$
			$\Delta H_{Zr-Al} = -44$
			$\Delta H_{Ni-Al} = -22$
15	Pt-Cu-P	Humps	$\Delta H_{Pt-Cu} = -12$
			$\Delta H_{Pt-P} = -35$
			$\Delta H_{Cu-P} = -18$
16	Pt-Ni-P	Shoulders	$\Delta H_{Pt-Ni} = -5$
			$\Delta H_{Pt-P} = -35$
			$\Delta H_{Ni-P} = -35$

**Figure 5.** Composition-dependent mean chemical affinity ΔH^{chem} for (a) $\text{La}_{70}(\text{Cu}_x\text{Ni}_{1-x})_{15}\text{Al}_{15}$ and $\text{Pd}_{40}(\text{Cu}_x\text{Ni}_{1-x})_{40}\text{P}_{20}$ MGs, and (b) $(\text{Cu}_{0.5}\text{Zr}_{0.5})_{100-x}\text{Al}_x$ MGs. The arrows indicate the directions along which β -relaxations become more pronounced with composition variations in each system [81] (Copyright 2013 Nature Publishing Group).

mechanism of chemical fluctuations, provides a quantitative way to predict the β -relaxation behavior in some MGs. It is noted that this correlation does not apply to $(\text{Cu}_{0.5}\text{Zr}_{0.5})_{100-x}\text{Al}_x$ systems, as shown in Fig. 5b—demonstrating that ‘fluctuations in the values of enthalpy’ are a more general argument.

In binary MGs, there is only one $\Delta H_{AB}^{\text{mix}}$ and thus no fluctuation to define. Intuitively, the fluctuation scenario should be reduced to a correlation between ΔH^{chem} and the β -relaxation behavior. Whether this correlation stands for different binary MGs has not been convincingly checked, because there are insufficient DMA data for binary MGs. However, recent results from Gao *et al.* (X.Q. Gao *et al.* unpublished) show that this correlation usually holds for many binary MGs, such as $\text{Cu}_{1-x}\text{Zr}_x$, $\text{Ni}_{1-x}\text{Zr}_x$, $\text{Cu}_{1-x}\text{Ti}_x$, $\text{Cu}_{1-x}\text{Hf}_x$, and $\text{Ni}_{1-x}\text{Nb}_x$, with different x , where MG ribbons can be prepared.

Similar chemical effects have in fact been observed in non-MG systems, such as organic glasses (molecular glasses and polymers). For example,

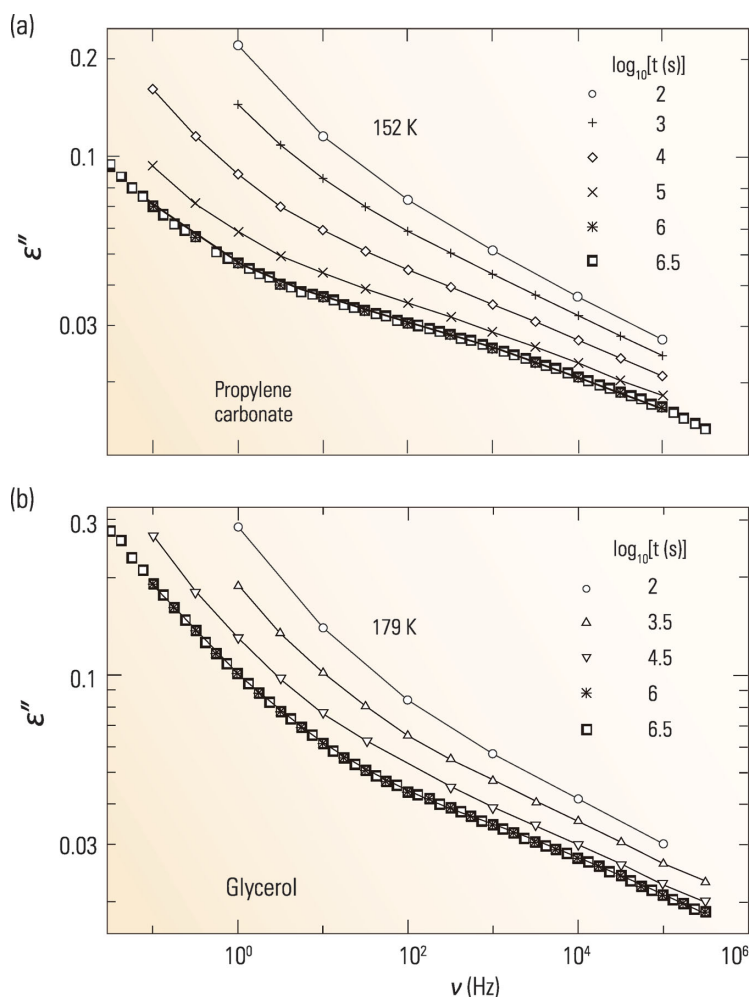


Figure 6. Aging effects on β -relaxation of **(a)** propylene carbonate and **(b)** glycerol for different aging times, measured by dielectric loss spectra [86] (Copyright 2000 American Physics Society).

Casalini *et al.* [72] used $-\text{SCH}_3$ to replace $-\text{OCH}_3$ groups in poly(methyl methacrylate) (PMMA) and found in their dielectric spectra that the intensity of the β -relaxation was substantially reduced because the electronegativity of sulfur is much less than that of oxygen. Their observations demonstrated that tuning the chemical interactions can result in different β -relaxation behavior in polymers, similar to the findings in MGs [81].

Mechanistically, these chemical effects on the β -relaxations in MGs (and hopefully in other types of glasses as well) can be understood, at least qualitatively, from the string model, [81] as discussed in the subsection entitled ‘String-like excitations in MGs’. In light of this scenario, it is reasonable that strong and comparable magnitudes of interactions among all the constituent atoms are needed to achieve the critical length of the string-like atomic configurations required for the β -events. On the contrary, weak interactions (or large fluctuations) between

certain atomic pairs would break the string-like configurations, making them less cooperative. Presumably, weakly bonded atoms diffuse readily, and thus act as ‘cutters’ or ‘anti-glue’ to the string. In other words, strong interactions hold neighboring atoms together to form the string-like configurations and to complete cooperative β -events.

Nevertheless, there remain some concerns with aspects of the effects of chemical composition and the ‘enthalpy fluctuation scenario’.

- (i) A currently known exception is the behavior of La/Ce–Cu–Al systems, where La–Cu–Al MGs have shoulder-like β -relaxations while Ce–Cu–Al MGs show excess wings, although La and Ce have similar values of enthalpy of mixing with Cu and Al. It is useful to study β -relaxations in different MG systems to carefully check the scenario of ‘fluctuations in the values of enthalpy’. In particular, exceptions may serve as new starting points for better understanding.
- (ii) Since the Miedema model is an empirical estimate, to obtain accurate values of enthalpy of mixing in a particular system, experiments or first-principles calculations are required.
- (iii) As well as this, the values of enthalpy of mixing might even be concentration dependent.
- (iv) Furthermore, this enthalpy of mixing-based approach does not consider the interactions between the same kind of atoms, which could be especially important for binary or monatomic systems and systems with high concentrations of solvent atoms.

Effects of thermal history and aging on the β -relaxations

Glasses exist in a non-equilibrium state, and almost all their properties are dependent on their thermal history, i.e. heat treatments such as aging or annealing, and heat/cooling rates [82–84]. There are numerous studies of the effects of thermal histories and aging on β -relaxation in molecular glasses, and a number of intriguing effects have been identified which have provided important insights into the nature and properties of β -relaxations [40,68,85–90].

By performing long-time aging experiments (up to five weeks), Schneider *et al.* [86] observed that the excess wings of two molecular glasses, propylene carbonate and glycerol, develop into shoulders during aging, as shown in Fig. 6. Their results provided convincing evidence that the excess wing, observed in a variety of glass formers, is in fact the high-frequency flank of a β -relaxation, and questioned the importance of the classification of ‘type A’ and ‘type B’ glass formers.

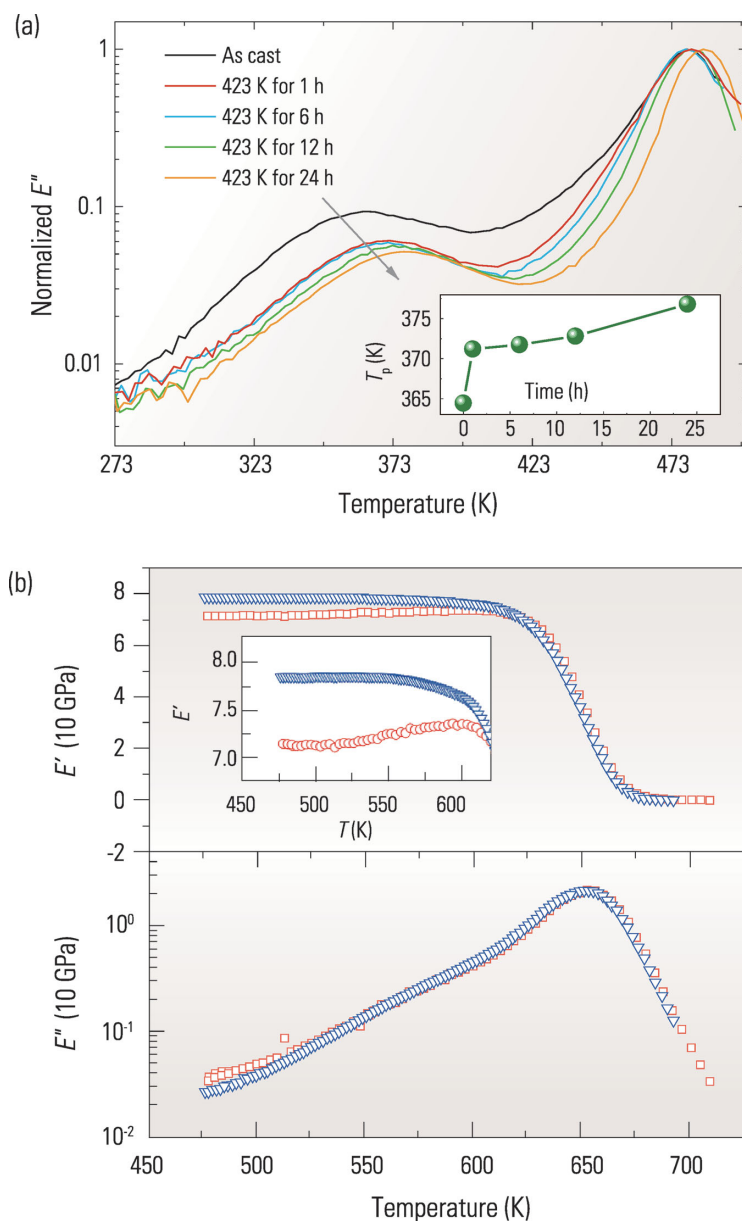


Figure 7. (a) Aging effects on β -relaxation of La-based MG [90]. (b) Effect of cooling rate on β -relaxation of Zr-based MG, measured by DMA loss spectra [89]; the blue triangles indicate as-cast MGs, while the red squares (circles, in the inset) indicate data measured at a cooling rate of 3 K/min (Copyright 2010 Wiley-VCH Verlag GmbH & Co. KGaA, Weinheim).

Aging and thermal history effects on β -relaxation in MGs have been addressed in several investigations. General observations can be summarized as follows.

- (i) Aging and slow quenching can reduce the intensity of β -relaxation in MGs with pronounced β peaks or humps, but cannot totally suppress the β -relaxation; a typical example is shown in Fig. 7a for a La MG [90].
- (ii) For MGs with β -relaxations that appear as excess wings, aging and slow quenching can make

these β -relaxations clearer, with shoulder-like features, as shown in Fig. 7b for a Zr MG [89] prepared at two different cooling rates. Note that this is mainly achieved by reducing the intensity of E'' below the wing regions, e.g. below 550 K in case of the Zr MG in Fig. 7b.

- (iii) Aging can increase E' (compared to that of as-cast MGs) at temperatures below the β -relaxations.

All these observations in MGs are consistent with those observed in non-MGs, like molecular glasses and polymers, suggesting that these are the universal features of β -relaxations in glassy states. Aging provides a physical means to tune the behavior of β -relaxations in MGs, although aging is less effective than modifying the chemical composition. It is noted that the studies on aging effects for MGs have been far from comprehensive, especially because crystallization of the MGs makes it impossible to examine long-term aging at relatively high temperatures [91]. On the other hand, long-time aging could yield significant information. For example, Cangialosi *et al.* [92] recently revealed a double-step enthalpy-recovery phenomenon at aging times as long as one year in some polymer glasses. Their results indicate the presence of two timescales for glass equilibration. Especially, the equilibration time of the first recovery step exhibits Arrhenius temperature dependence while the second step shows super-Arrhenius behavior, and these two merge together at higher temperatures—in much the same way as the temperature-dependent β - and α -relaxation times.

Finally, we mention that there are some other means to tune β -relaxations in non-MGs, such as modifying the functional groups in organic glasses [72], changing the chain length of molecular glasses (going from oligomers to polymers) [93,94], copolymerization and mixing [95–99], crosslinking [100], and varying molecular weights and distributions. All of these are only possible because of the complex molecular structures of organic materials [94]. However, another method, i.e. applying high pressure [101–106] to glass-forming liquids, could potentially be of interest in the study of β -relaxations in MGs; modifications of currently available measuring facilities would be required.

POSSIBLE MECHANISM OF β -RELAXATION AND SOME CONTROVERSIAL PERSPECTIVES

The actual degrees of freedom involved in β -relaxation have not been clearly identified. Discovering the mechanism is not only a central problem in studies of β -relaxations, but also one of

the most challenging issues in glassy physics [11]. Although there are several models and hypotheses, controversy remains about the mechanism of β -relaxation. Here we review these contentious points of view, paying particular attention to insights gained from MGs.

Homogeneous versus inhomogeneous

Johari first suggested that β -relaxation was a local motion in loosely packed isolated regions [21,22]. These regions were referred to as ‘islands of mobility’ or ‘defects’, in a mechanically rigid structure of a glass [21,22]. This picture, however, does not specify what these regions are or the temperature dependence of their sizes. In MGs, such regions were intuitively assigned to regions of lower density and reduced mechanical stiffness [107]. Johari’s picture, in a sense, is a spatially inhomogeneous scenario, where only a small fraction of atoms take part in the motions associated with the β -relaxations. On the other hand, Williams and Watts proposed an alternative view that β -relaxation is due to the motion of ‘essentially all molecules with a nearly temperature independent small angle’ [108,109]. Both these scenarios find some support from experimental results. Specifically, the solvation dynamics observations of Wagner and Richert [110] have indicated that the atomic motions associated with β -relaxation in a D-sorbitol liquid occur in a spatially uniform manner. Some NMR results also support the spatially homogeneous scenario [111–114]. However, Johari noticed that when several properties were examined together (especially aging and densification effects), the homogeneous scenario is not favored [22]. By considering the correlation between β -relaxation and diffusions in MGs, Yu *et al.* suggested that it is unlikely that all the atoms take part in the β -relaxation in MGs [115].

On the other hand, the heterogeneous dynamics of the α -relaxation have been established in recent years [116–118]. One important class of methods are those that examine ‘non-linear dynamics’; examples of these approaches are multidimensional NMR, dielectric spectra ‘hole-burning’ [119,120], large field dielectric spectra [121,122], microwave heating [123], and aging dynamics [124,125]. In principle, these appealing methods can be transferred to study the β -relaxations, although there have only been a few such attempts.

Cooperative versus non-cooperative

The β -relaxation was initially considered to be a non-cooperative process. However, some recent studies

have demonstrated that the β -relaxation must involve some degree of cooperativeness. By mixing toluene with other molecular liquids, Micko *et al.* [126] found that there is a threshold concentration, and below this ($\sim 75\%$ of toluene) the relaxation strength and dynamics of the β -process change abruptly. Similar behavior was also observed by Yu *et al.* [44] in a systematic study on La/Ce-based MGs (see the section entitled ‘CORRELATIONS BETWEEN β -RELAXATION AND α -RELAXATION’). These results provide strong arguments for the β -relaxation in molecular and MGs being cooperative. However, it is not clear whether this conclusion stands as a general rule for all glass-forming materials.

Translational versus reorientational motion

In some organic glass-forming materials, the molecular motions associated with β -relaxations were considered as reorientational jumps of molecules. This view was particularly substantiated in plastic crystals [127,128]. Those materials are composed of weakly interacting molecules possessing reorientational or conformational disorders while the translational degrees of freedom are frozen as crystalline states. Obviously, such a mechanism cannot be directly applied to MGs, since there is no reorientational degree of freedom of atoms, which is the basic ‘building block’ in MGs. These differences, if cannot be properly reconciled, question the existence of a universal interpretation of the mechanism of β -relaxations in various glass-forming materials [128].

Length scale

The typical length scale associated with β -relaxations has been suggested to range from very local (the first atomic shell) to quite extended (several tens of nanometers) by different authors [11,43,126,129,130]. For MGs, by identifying that β -relaxations and shear transformation zones (STZs) have the same activation energy, Yu *et al.* first assumed that β -relaxations could take place in spherical regions containing approximately 200 atoms [43]. In a Pd–Cu–Si MG, Bedorf and Samwer [129] studied the effects of length scale on relaxations and found that by reducing the film thickness to < 30 nm the β -relaxations were effectively suppressed, and therefore the length scale associated with β -relaxations should be of the same order (or smaller). On the other hand, the composition-dependent β -relaxations in molecular

glasses studied by Micko *et al.* [126] seem to indicate a rather small correlation length, and apparently a certain minimal local concentration is sufficient for a given molecule to exhibit β -relaxation in the glassy state.

Potential energy landscape perspective

Stillinger suggested that β -relaxations correspond to rearrangements of the system between neighboring potential energy minima, while α -relaxations involve a series of such rearrangements in cooperative manner, which move the configurations from one megabasin of the potential energy surface (PES) to another [131]. Since the overall activation energy is larger for the α -relaxations, they would be frozen out at higher temperatures, while β -relaxations can survive to very low temperature. Such a descriptive picture is consistent with experimental observations. By modeling the PES of the β -relaxation as an asymmetric double-well potential, Dyre [132] successfully explained the hysteresis of the dielectric β -loss peak frequency and magnitude during cooling and reheating through the glass transition of tripropylene glycol. In MGs, there is a cooperative shear model (CSM), which relates the PES, α - and β -relaxations, and mechanisms of plastic deformation of MGs. The CSM is discussed in the section entitled 'Relating β -relaxations to activation of STZs'.

Tanaka's model and emergence of rigidity

In 2004, Tanaka [133] proposed a phenomenological microscopic model of β -relaxation from the perspective of local reorientational fluctuations. In this model, α -relaxations correspond to the creation and annihilation of metastable islands in supercooled liquids, while β -relaxations correspond to a kind of restricted, jump-like, reorientational, and vibrational motion within these solid-like metastable islands. One prominent feature of Tanaka's model is that the existence of solid-like metastable islands is a prerequisite for the existence of β -relaxations.

Saito *et al.* [134] recently mapped the relaxation times of inter- and intramolecular correlations in *o*-terphenyl using a quasi-elastic scattering method. They found that the β -process is decoupled from the α -process at 278 K; this temperature is clearly below the previously known decoupling temperature of 290 K, at which the α -relaxation dynamics change. They concluded that a sufficiently solid-like condition, achieved by further cooling from 290 K, is required to decouple the β -process from the α -process. Their results seem to support Tanaka's model.

String-like excitations in MGs

Recently, based on the random first-order transition theory [135], Stevenson and Wolynes [136] proposed a universal origin for secondary relaxations in supercooled liquids and glasses. They showed that the α -relaxation takes place through activated events involving compact regions, while the β -relaxation is governed by more ramified, string-like, or percolation-like clusters of particles. Samwer *et al.* adapted this concept to MGs, incorporating it with a CSM [137–139], and further suggesting that a β -event can be considered as a string of atoms that moves back and forth reversibly and cooperatively within the confinement of the surrounding elastic matrix [129]. This suggestion has been applied to interpret the observed chemical effects on β -relaxation [81] and the correlation between β -relaxation and diffusion of the smallest atoms in MGs [115]. By molecular dynamics (MD) simulation of a real DMA experiment, Cohen *et al.* [140] recently showed that randomly pinning only a small fraction of atoms ($\sim 2\%$), and not allowing them to participate in the relaxation dynamics, can strongly suppress the β -relaxations in a model 2D Lennard–Jones glass. Such a result supports the idea that β -relaxation is related to the motions of string-like configurations. Although string-like excitations have been inferred in some simulations [140–142], there is still no direct experimental evidence for this model.

CORRELATIONS BETWEEN β -RELAXATION AND α -RELAXATION

One important reason for the theoretical interest in studying β -relaxations in glass-forming materials is that recently their connections to the central challenge of glassy physics, the nature of the glass transition [5,12], have been revealed. Traditionally, α -relaxation was believed to be mainly responsible for the glass transition phenomenon, while the β -relaxations, which occur at shorter times or lower temperatures, were thought to play an unimportant role in glass transitions. However, many recent findings have demonstrated that β -relaxations are connected to α -relaxations or glass transitions; in fact, β -relaxation can be considered the dynamical precursor of α -relaxation [5,11,12]. This topic is now being actively discussed in different kinds of glass-forming materials and has been explained theoretically by a coupling model of Ngai. Specifically, the coupling model predicts quantitatively the locus of the β -relaxation on the relaxation spectrum from knowledge of the corresponding α -relaxation [5,11,12]. At any temperature T and pressure P , there is a general relationship between the

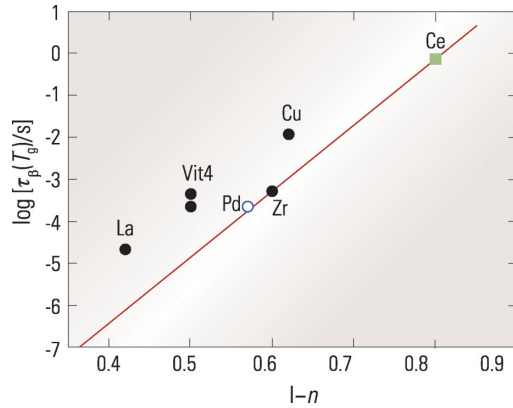


Figure 8. Connection between $\log[\tau_\beta(T_g)]$ and $\beta_{\text{KWW}} \equiv (1-n)$ of the Kohlrausch–Williams–Watts correlation function used to characterize the frequency dispersion of the α -relaxation. See [143] for the meanings of the labels (Copyright 2013 American Institute of Physics).

α -relaxation time $\tau_\alpha(T, P)$ and the β -relaxation time $\tau_\beta(T, P)$ [5,12]:

$$\log[\tau_\alpha(T, P)/\tau_\beta(T, P)] \approx n \log[\tau_\alpha(T, P)/t_c], \quad (3)$$

where $n(T, P)$ is the complement of the stretch exponent, $\beta_{\text{KWW}} \equiv (1 - n)$, of the Kohlrausch correla-

tion function of the α -relaxation in the time domain $\varphi(t) = \exp[-(t/\tau_\alpha)^{1-n}]$, while t_c is a crossover time from uncorrelated (short-time) to correlated (long-time) dynamics and is about 0.2 ps for MGs or about 2 ps for molecular glasses. Recently, Ngai *et al.* [143] reported that Equation (3) holds reasonably well for MGs (see Fig. 8). Note also that at ambient pressure and T_g , if we define $\tau_\alpha = 100$ s (or some other arbitrary value), Equation (3) reduces to a relationship between τ_β and n , as seen in Fig. 8. Also, Equation (3) is well established in many molecular glass formers [12].

Equation (3) has also implications for understanding the separation of α - and β -relaxations, i.e. the excess wing and peak problem. At specific T and P , Equation (3) indicates that the magnitude of $\tau_\alpha(T, P)/\tau_\beta(T, P)$ is dependent on n . For an extremely small $n \rightarrow 0$, the difference between τ_α/τ_β would be too small to be distinguished and these two relaxations should be coupled together, i.e. the excess wings should occur. Although n is hard to obtain accurately in MGs (due partly to the rapid crystallization of their supercooled liquids), considering that n and fragility m could be correlated in MGs with nearly similar compositions, Yu *et al.* [11,44] recently demonstrated a correlation between the behaviors of β -relaxation and m in a systematic study on $(\text{Ce}_x\text{La}_{1-x})_{68}\text{Al}_{10}\text{Cu}_{20}\text{Co}_2$ (where $0 \leq x \leq 1$) MGs, as displayed in Fig. 9a–d. In this system, the Ce-rich MGs have small values of fragility and show β -relaxations as excess wings, while the La-rich ones have larger fragilities and show β -relaxations as humps; both the fragilities and shape of the β -relaxations change systematically with x . In addition, Fig. 9b and d shows that the curves for β -relaxation and fragilities as a function of composition adjustments are sigmoidal, indicating a clear transition. This may be a sign that the β -relaxation is cooperative in nature. The structures and dynamics of the MGs change drastically with alloying [11]. However, a clear understanding of the relationships between atomic structures and relaxation dynamics in glassy materials has still not been reached [11].

On the other hand, we know that chemical fluctuations correlate with β -relaxation behavior. It will be an interesting topic to investigate the relationships among m , n , and enthalpies of mixing and β -relaxation behavior in MGs.

Over the past decade, E_β values for many MGs have been determined [11,13,43,59]. An approximately linear relationship between E_β and T_g was obtained [11,43] and see Fig. 10:

$$E_\beta = 26(\pm 2)RT_g. \quad (4)$$

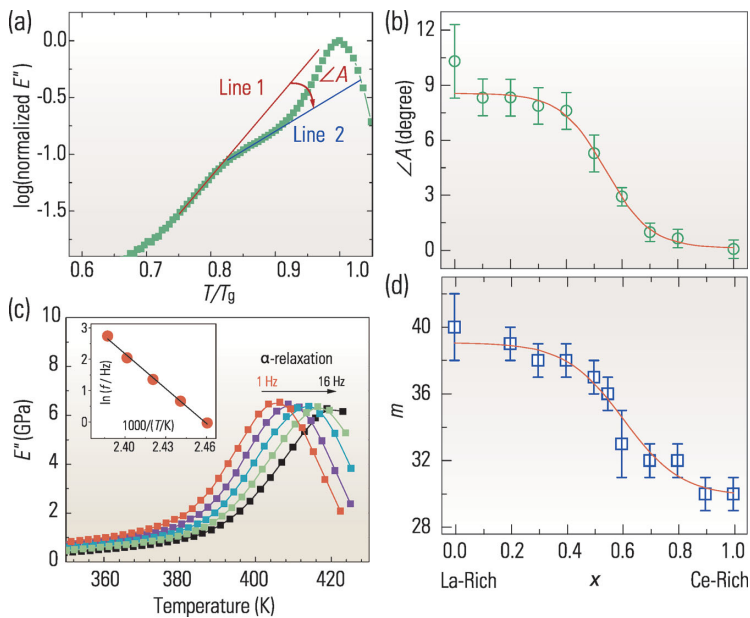


Figure 9. Correlation between β -relaxation and fragility in $(\text{Ce}_x\text{La}_{1-x})_{68}\text{Al}_{10}\text{Cu}_{20}\text{Co}_2$ MGs. **(a)** The definition of ΔA that characterizes the obviousness of the β -relaxation humps, with $x = 0.2$ as an example. **(b)** The dependence of ΔA on x . **(c)** E'' data showing the α -relaxation (test frequencies are 1, 2, 4, 8, and 16 Hz, from left to right) for $x = 0.2$; the inset is an Arrhenius plot of α -relaxation peaks of the MG, from which fragility m can be extracted. **(d)** The dependence of m on x . Adapted from [11] (Copyright 2013 Elsevier Ltd).

As T_g is the characteristic temperature that signals the arrest of the α -transition, this relationship can be considered as further evidence of the correlation between β -relaxation and α -relaxation (or glass transitions). Within the coupling model, there is a similar relationship between E_β and T_g , as demonstrated by Ngai and Capaccioli for organic glass-forming materials [144]. We will not discuss correlations between α - and β -relaxations in MGs in further detail, as this topic is far less explored in MGs.

CORRELATIONS BETWEEN MECHANICAL PROPERTIES AND β -RELAXATION IN MGs

Deformation of MGs and STZs

Mechanical properties of MGs are of great interest to the materials science community [145–147]. Macroscopically, deformation of MGs is highly temperature and strain rate dependent. At low temperatures and high strain rates, deformation is essentially localized in some thin layers, called shear bands (which have estimated thicknesses of ~ 10 – 100 nm) [148]. At higher temperatures, especially within the supercooled liquid regions, MGs can be deformed homogeneously, either by non-Newtonian or Newtonian flow depending upon temperature and strain rate [145–147].

The deformation mechanism of MGs (or any other disordered system) is not well understood [145–147]. This is in sharp contrast to that in crystalline materials. In crystalline materials, mechanical properties and deformation mechanisms can be well explained on the basis of atomic and electronic structures plus lattice defects, such as dislocations, twins, crystal boundaries, and so on. The deformation mechanisms of crystalline materials have become one of the most well understood physical subjects, where physics has enjoyed great success, and upon which modern materials science has been built [149]. In MGs, however, the atomic structure is disordered and there is no reference lattice to which lattice defects can be related. The deformation mechanisms of glassy materials are an outstanding challenge in condensed matter physics and materials science.

Microscopically, the deformation of MGs is proposed to be accommodated by plastic rearrangements of atomic regions involving several tens or hundreds of atoms, termed STZs or, more generally, ‘flow units’ [150–153]. The STZ, as revealed by computer simulations and observed in colloidal systems, is essentially a group of atoms within a rela-

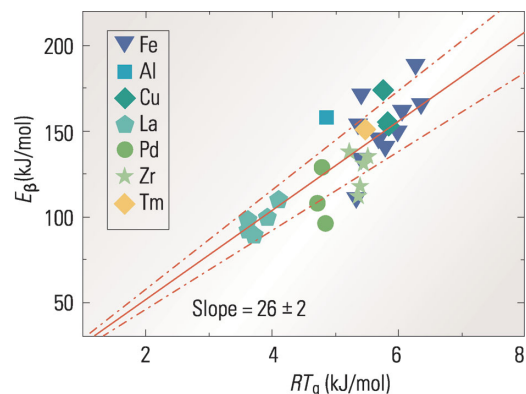


Figure 10. Relationship between E_β and RT_g for different MGs; the lines are least-squares linear fits [11].

tively loosely packed region that undergoes an inelastic distortion from one configuration to another, crossing an energy barrier. Such an apparently simple definition hides considerable complexity, and various fundamental questions about STZs remain open, including the geometrical and structural aspects of potential STZs, their activation mechanisms, and how STZ events evolve into shear banding [11,145–147,150–153].

Relating β -relaxations to activation of STZs

Recently, there is growing interest in the connections between the mechanisms of plastic deformation and the relaxations of MGs [11,35,43,137–139]. On the basis of Frenkel’s analysis of shear strength for a dislocation-free solid, Johnson and Samwer proposed a CSM to study the deformation mechanisms in MGs [137–139]. In the CSM, deformation and flow are modeled as activated hopping between inherent states across energy barriers that are assumed to be, on average, sinusoidal. This treatment gives rise to a functional relationship between viscosity and isoconfigurational shear modulus G , leading to rheological laws describing the Newtonian and non-Newtonian viscosity of MG-forming liquids over a broad range of rheological behavior. In the CSM, the potential energy barrier of an STZ is given as [137–139]

$$W = (8/\pi^2)G\gamma_c^2\zeta\Omega, \quad (5)$$

where Ω is the average volume of an STZ, γ_c the average elastic limit, and ζ a factor arising from the matrix confinement of an STZ. The CSM was originally introduced to elucidate the temperature dependence of yield strength, yet it has also been shown to provide an effective interpretation of many aspects of mechanical behavior of MGs.

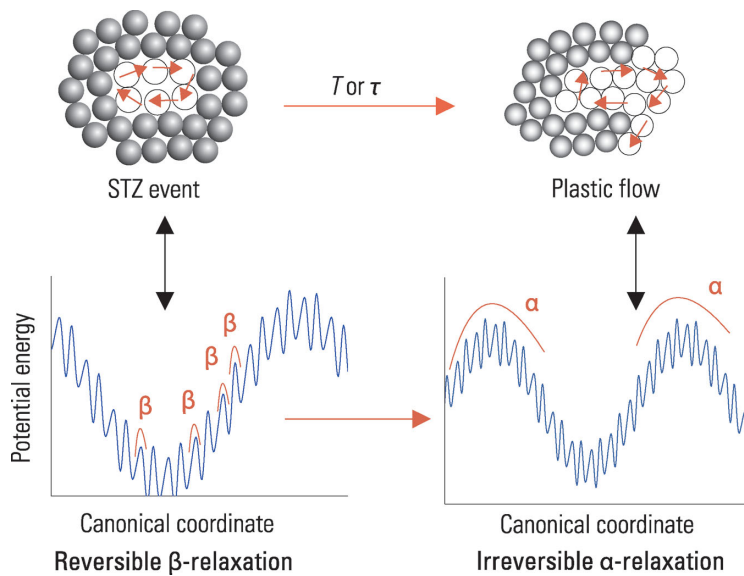


Figure 11. 2D schematic illustration of β -relaxation (STZ activation, top-left panel), α -relaxation (flow and yielding, top-right panel), and their corresponding potential energy landscapes (bottom panel). The filled circles represent atoms with low propensity for motion, while the open circles represent atoms with high propensity for motion. The red/bold arrows indicate the possible motions of atoms. The β -relaxation (potential STZ event) is localized with a cooperative nature, and is reversible because the atoms are confined by their surroundings, while α -relaxation (percolation of STZs, or plastic flow and yielding) incorporates large-scale atomic migration and is irreversible.

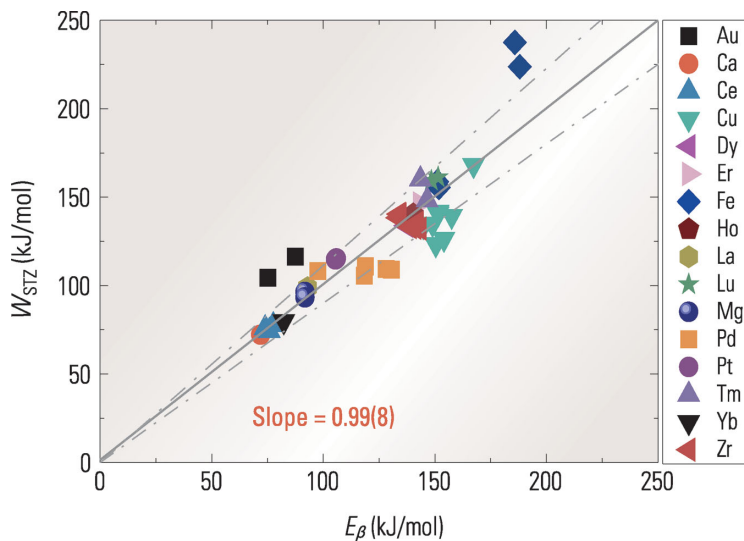


Figure 12. Relationship between E_β and W_{STZ} [11] (Copyright 2013 Elsevier Ltd).

From the CSM, Harmon *et al.* [138] firstly suggested that the isolated STZ events confined within the elastic matrix are associated with β -relaxations, while percolation of these transitions, leading to the collapse of the confining matrix and breakdown of elasticity, is associated with the α -process. A 1D schematic drawing of a potential energy landscape illustrating their concepts is presented in Fig. 11.

Direct experimental evidence about the relationships between STZ events and β -relaxations was given by Yu *et al.* [11,43]. From their measured values of G and estimated values of Ω for more than 40 kinds of MGs, the molar potential energy barrier of an STZ, W_{STZ} , has been estimated as

$$W_{\text{STZ}} \equiv N_0 W \approx 0.39 G V_m, \quad (6)$$

where N_0 is the Avogadro constant and V_m the molar volume. A remarkable finding is that, as shown in Fig. 12, W_{STZ} and E_β are almost equivalent to each other in all known MGs, i.e.

$$W_{\text{STZ}} = E_\beta. \quad (7)$$

This equality was further verified to hold in individual systems of MGs, such as Zr-, Cu-, Fe-, or rare-earth-based MGs, demonstrating that activation of STZs and the β -relaxations are directly correlated.

The correlation between β -relaxations and activation of STZs is also supported by molecular simulations. For example, Rodney and Schuh [154] simulated the shear deformation of a 2D $\text{Cu}_{50}\text{Zr}_{50}$ MG and obtained spectra of activation energies of STZs. For the undeformed MG, a peak is centered at about 0.72 eV (corresponding to ~ 70 kJ/mol) indicating that $W_{\text{STZ}} \sim 70$ kJ/mol. For bulk $\text{Cu}_{50}\text{Zr}_{50}$ MGs, E_β can be estimated (from Equation 4) to be $E_\beta \approx 26RT_g \sim 150$ kJ/mol. Glass transition theory also predicts a lowering of the surface activation energy by a factor of 2 from that of the bulk [155]; this implies that $E_\beta \sim 75$ kJ/mol for the 2D $\text{Cu}_{50}\text{Zr}_{50}$ MG. Such a value is very close to the $W_{\text{STZ}} \sim 72$ kJ of Rodney and Schuh [154]. For a deformed MG, W_{STZ} decreases, indicating a change in the glass structure and tilting of the potential energy landscapes. Although this comparison is very rough and deserves further clarification, it has important implications, as this conclusion depends on neither the CSM nor on the geometry of the STZs.

Correlations between deformability, β -relaxations, and activation of STZs

Since STZs are generally considered to be the basic structural units of deformation in glassy solids, analogous to dislocations in crystalline materials, it is of practical importance to see how the properties of STZs affect the mechanical properties of MGs. Generally, two properties of STZs have been evoked to explain the different mechanical behavior of MGs: the activation energy W_{STZ} and the volume of an individual STZ, Ω_{STZ} .

Poisson's ratio ν , when plotted against $W_{\text{STZ}} = E_\beta$ for many Au-, Pd-, Pt-, Zr-, Cu-, Fe-, and

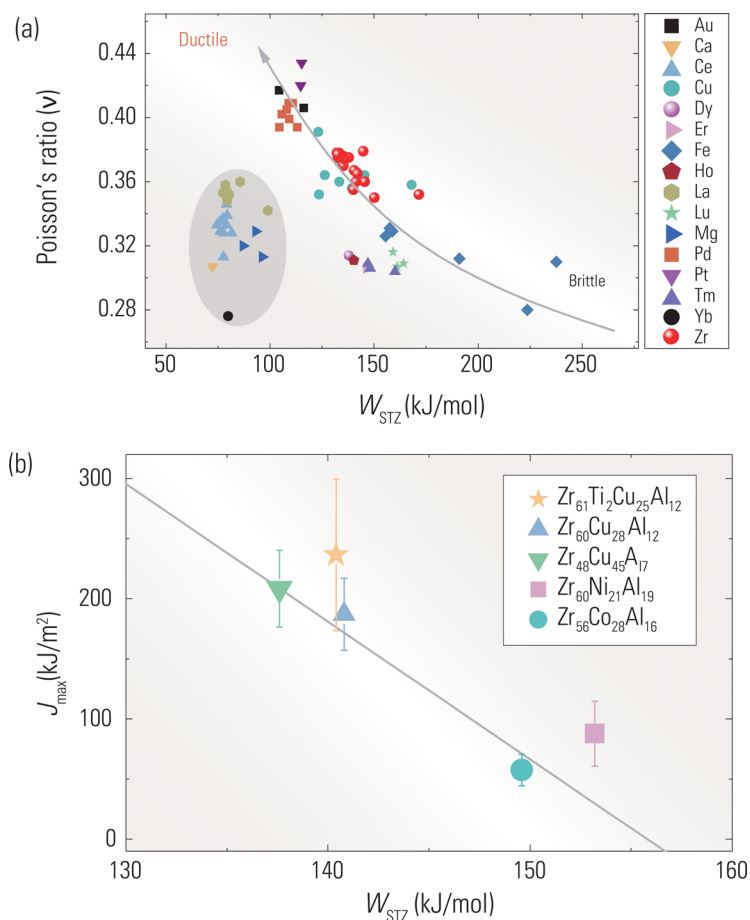


Figure 13. Correlations between (a) W_{STZ} and Poisson's ratio [42] (Copyright 2010 American Physics Society). (b) W_{STZ} and fracture tolerance J_{max} , redrawn using data from [157] (Copyright 2011 Acta Materiala Inc.).

some late-rare-earth-based MGs in Fig. 13a [11,43], demonstrates yet another correlation between these quantities. This result has important implications for mechanical properties of MGs because Poisson's ratio is an indicator of ductility. Thus, the β -relaxations, like the STZs, are fundamental aspects of plasticity, yield stress, and ductility of MGs. Lower W_{STZ} means that STZs are easily activated, and thus the corresponding MGs show better ductility and toughness. Exceptions to this correlation are found for some MGs based on Ca, Ce, Yb, and Mg, shown in the box in Fig. 13a. Yu *et al.* [11,43] suggested that this is caused by the low T_g (near to or possibly lower than room temperature, at which MGs are fabricated and kept) and/or low oxidation resistance of these MGs, and that processes such as physical aging and oxide deterioration are involved. This suggestion was recently confirmed by Madge *et al.* [156]. They showed that the Mg-, La-, and Ce-based glasses are very prone to oxidation and that their limited oxygen solubility always leads to oxide inclusions in the glassy matrix, thus drastically

decreasing fracture toughness. If these factors are carefully avoided, these MGs are in fact much tougher. Fig. 13b [157] shows the maximum strain energy release rate J_{max} , which is a direct measure of fracture toughness, for some Zr-based MGs, as measured by He *et al.*; these J_{max} values correlate well with W_{STZ} , demonstrating again that W_{STZ} can be an indicator of macroscopic mechanical properties.

There are intriguing perspectives on the relationship between the volume of STZs and the ductility of MGs [158,159]. By performing nanoindentation experiments, Pan *et al.* [158] characterized the size of STZs in some typical MGs. They reported that the ductility of BMGs is correlated with their STZ volumes, as shown in Fig. 14a. They suggested that a large STZ volume, compared with a smaller one, means that fewer STZs need to be activated to nucleate a shear band, and these large-size STZs during plastic deformation can produce large internal concentrations of applied stress where thermally activated production of new flow becomes easy. On the other hand, Liu *et al.* [159] took measured values of E_β for MGs and used them as W_{STZ} to obtain the STZ volume from the CSM model, via Equations (4), (5), and (7). Their results, as shown in Fig. 14b, indicated that ductility and STZ volumes are anti-correlated, in contradiction to the results of Pan *et al.* [158]. Liu *et al.* [159] suggested that a smaller STZ, when compared with a larger one, enables more STZs to be activated for the nucleation of more shear bands, and promotes the formation of multiple shear bands and larger plasticity in MGs. These two conflicting results indicate that the relationship between ductility and volume of STZ is still unclear. As well as this, the complicated geometry of STZs under large stress/strain as revealed by simulations and experiments in colloidal glasses makes it more difficult to examine the correlation between geometry of STZs and ductility of MGs. The energies, W_{STZ} and E_β [11,43], and other features of β -relaxations, are likely to be more important in the mechanisms of plastic deformation of MGs.

Achieving tensile ductility in MGs by activation of β -relaxations

Regarding the mechanical properties, a serious drawback of MGs is their brittleness. Some MGs show considerable plastic strain under constrained deformations, such as compression and bending; however, the unconstrained tensile plasticity of MGs is almost nil [145–148]. Although substantial efforts have been made to enhance the tensile ductility of MGs, it is still an outstanding challenge to obtain MGs with macroscopic tensile ductility at room

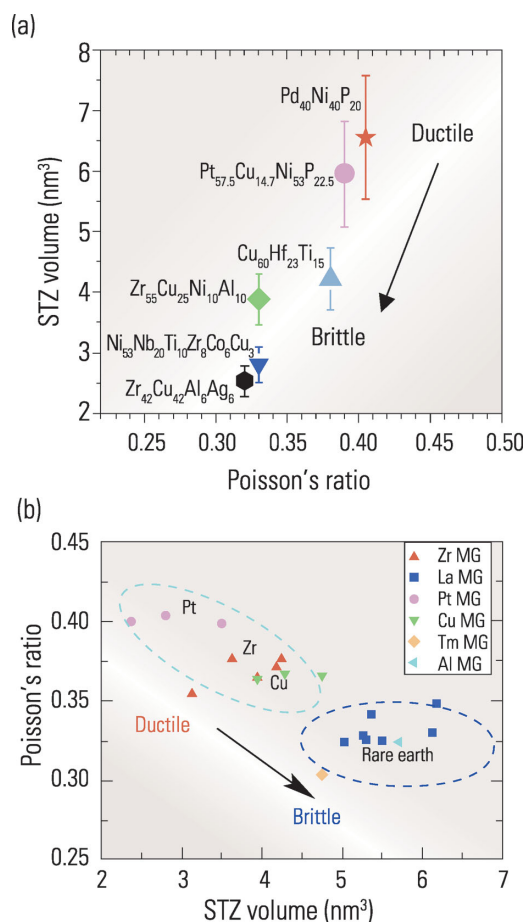


Figure 14. Relationship between Poisson's ratio and volume of STZ **(a)** from nanoindentation measurements of Pan *et al.* [158] (Copyright 2008 National Academy of Sciences, USA) and **(b)** inferred from β -relaxation data of Liu *et al.* [159] (Copyright 2012 Acta Materiala Inc.).

temperature. Meanwhile, the lack of tensile plasticity also hinders studies on some fundamental issues, such as the mechanisms of plastic deformation.

Recently, insights from the correlations between β -relaxation and STZs were exploited to successfully mitigate the brittleness of MGs [35]. The idea is straightforward: as β -relaxation is related to the activation of STZs, one could expect that MGs with pronounced β -relaxations at relatively low temperatures might be macroscopically ductile. The La-based MGs, presented in Fig. 2a, are such candidates. In a $\text{La}_{68.5}\text{Ni}_{16}\text{Al}_{14}\text{Co}_{1.5}$ MG, macroscopic tensile plasticity has indeed been achieved at and near room temperature by the activation of the β -relaxation, as shown in Fig. 15 [35]. Besides, the mechanical properties of the La MG are strain rate dependent. As demonstrated in Fig. 16, tensile plastic strain begins to appear at about 313 K when the strain rate is $1 \times 10^{-5} \text{ s}^{-1}$, but does not appear until about 323 K at $1 \times 10^{-4} \text{ s}^{-1}$; the temperature

for plastic strain increases to about 343 K when the strain rate is $1 \times 10^{-3} \text{ s}^{-1}$. Fig. 17a summarizes the temperature–strain rate deformation map, and reveals a clear ductile-to-brittle transition (DBT). Remarkably, the β -relaxation and DBT follow similar temperature–frequency dependence in an Arrhenius plot, as shown in Fig. 17b. Furthermore, the deformation and fracture morphologies, as shown in Fig. 17c and d, confirm the ductile nature of the MG when the β -relaxation is activated. These results demonstrate that β -relaxation and DBT share the same dynamics, and the activation of β -relaxations is a necessary condition to achieve tensile plasticity in MG. It also suggests that mechanical properties can be understood and even predicted from the perspective of β -relaxations [35].

Fig. 18 compares the mechanical behavior of the La MG with some other typical MGs in a deformation map [35]. It clearly shows that the La-based MG has tensile ductility in its glassy state, in sharp contrast to many other currently known MGs, for which brittleness is maintained very close to T_g , even in constrained (compressive) deformation. For example, Cu-, Zr-, and Ti-based MGs [160–166] show exclusively brittle behavior from $0.7T_g$ to $0.9T_g$, and Ce-based MGs [164], with similar T_g to La MG, are purely brittle, even at a test temperature of $0.92T_g$ and strain rate of 10^{-4} s^{-1} . An Sr MG [164], with even lower $T_g \approx 323\text{K}$ (its β -relaxation curve is excess wing), shows its DBT at a higher scaled temperature, that is associated with its α -relaxation. This comparison confirms that the tensile ductility of the La MG is due to its pronounced β -relaxation at relatively low temperatures, rather than to its low T_g .

To further demonstrate the deformability of MGs with different β -relaxations, Wang *et al.* [167] recently conducted a comparative study, as shown in Fig. 19. The $\text{La}_{70}\text{Ni}_{15}\text{Al}_{15}$ MG exhibits a pronounced β -relaxation peak as well as impressive tensile elongation when deformed at $0.75T_g$, where its β -relaxation is activated. On the other hand, the $\text{Cu}_{45}\text{Zr}_{45}\text{Ag}_{10}$ MG shows only an ‘excess wing’ β -relaxation, merged with the α -relaxation, and its tensile elongation is negligible when deformed at $0.75T_g$. Their results confirm that the β -relaxation, when activated, is a good indicator of the mechanical properties, as firstly suggested by Yu *et al.* [35].

As well, the relationship between β -relaxation and DBT, shown in Fig. 17b, may suggest some fundamental aspects of the deformation mechanisms of MGs. In a wide range of crystalline materials, the apparent activation energy of the DBT is equal to the activation energy for dislocation glide (known as the Peierls stress), clearly demonstrating that in crystalline materials the underlying mechanism of DBT is controlled by the mobility of

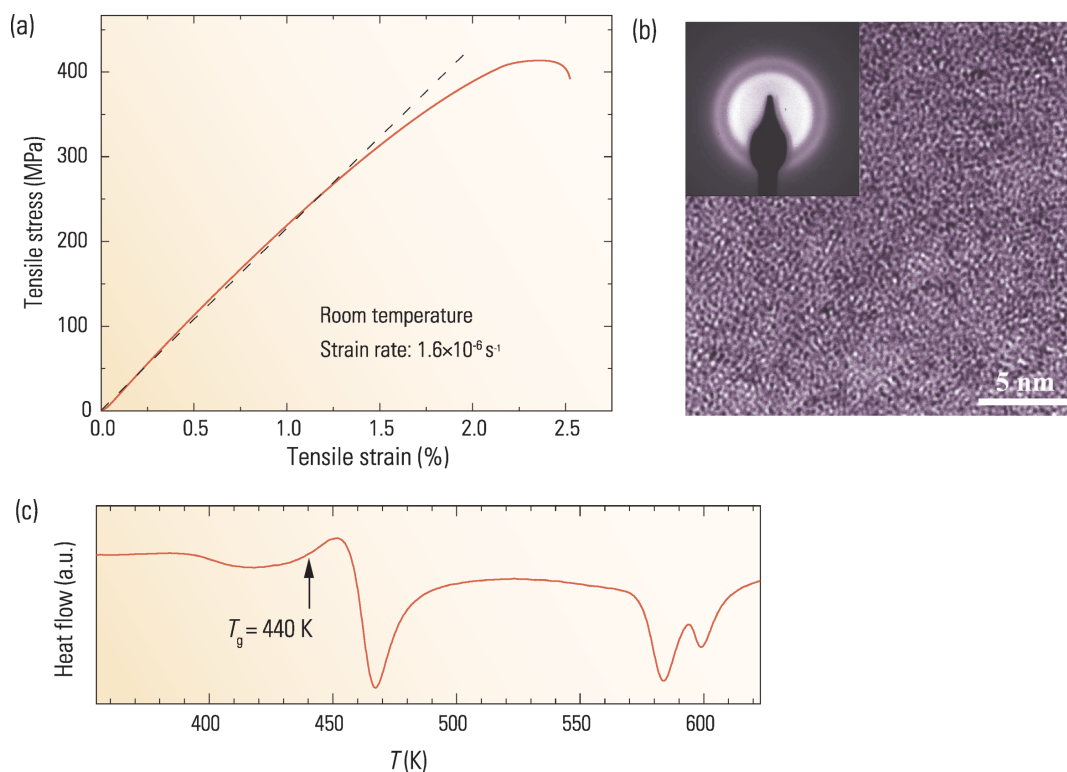


Figure 15. (a) Tensile stress–strain curve, (b) HRTEM with (inset) nanodiffraction, and (c) thermal properties measured by DSC of a La_{68.5}Ni₁₆Al₁₄Co_{1.5} MG.

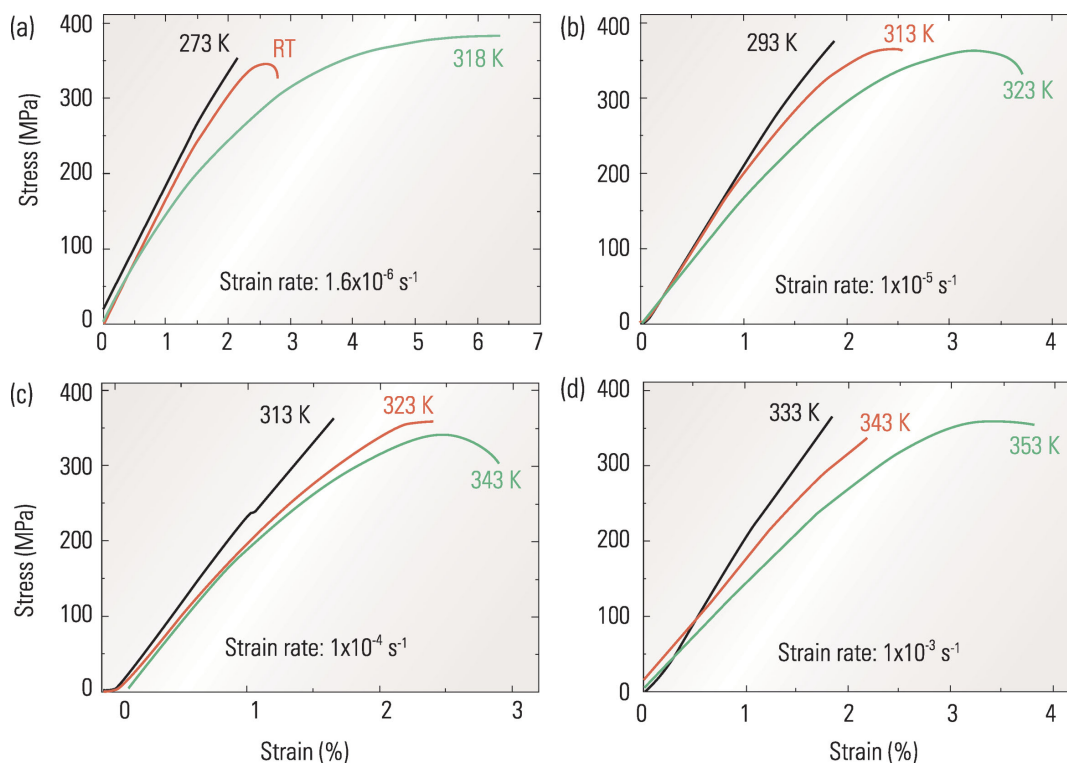


Figure 16. The engineering stress–strain curves (in tension) of a La MG tested at strain rates (a) $1.6 \times 10^{-6} \text{ s}^{-1}$, (b) $1 \times 10^{-5} \text{ s}^{-1}$, (c) $1 \times 10^{-4} \text{ s}^{-1}$, and (d) $1 \times 10^{-3} \text{ s}^{-1}$ [35] (Copyright 2012 American Physics Society).

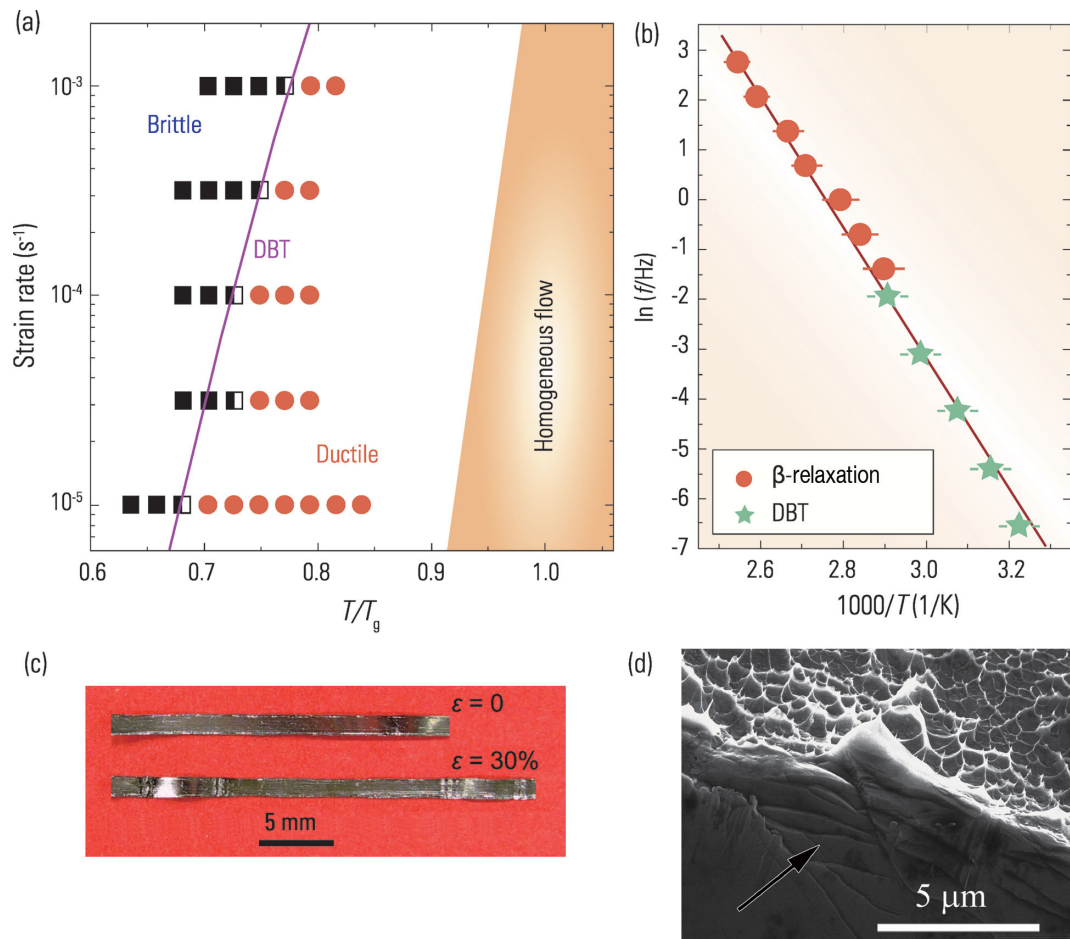


Figure 17. (a) Deformation mode map summarizing tensile tests at different temperatures and strain rates, see [35] for the meanings of the symbols. (b) Arrhenius plot of DBT and β -relaxation of the MG. (c) Image of the MG before and after tensile testing. (d) SEM image of a La MG ductile fracture surface (Copyright 2012 American Physics Society).

dislocations [168,169]. In the case of MGs, the activation energies for STZ formation and β -relaxation are similar, meaning that one can infer that the DBT of MGs is closely related to the activation of STZs as well as the β -relaxation. However, deep connections between DBT and the motions of deformation units (dislocations in crystalline materials or STZs in MGs) are not established. Nevertheless, it is an attractive prospect to incorporate insights from β -relaxations to design new materials with superior properties.

Manifestations of β -relaxation under creep and stress relaxation

Creep and stress relaxation describe how materials relieve strain/stress under constant stress/strain as a function of time, and have also been studied to shed light on the deformation mechanisms of MGs [170–176]. Park *et al.* [172] reported that elastostatic compression (i.e. compressive creep at low stress level)

imposed on MGs at room temperature could enhance their subsequent compressive plasticity. They initially attributed this observation to some kind of irreversible structural disordering induced by creep. Sandor *et al.* [173] found, from elaborate NMR measurements, that creep can induce atomic processes that lead to changes in local site symmetry at Al sites in a La–Ni–Al MG. Sandor *et al.* [173] also estimated the activation energy of such processes; interestingly, their activation energy value matches well with the activation energy of β -relaxation in the same MG.

In a long-time stress relaxation measurement, Jiao *et al.* [174] observed double power-law behavior of the decaying stress, as shown in Fig. 20a and b. They suggested that such a transition indicates a crossover from stochastic activation to self-organized cooperative motion of STZs. On the other hand, we can demonstrate here that such a transition, in essence, is a manifestation of the β -relaxation. For the $\text{Zr}_{52.5}\text{Ti}_5\text{Cu}_{17.9}\text{Ni}_{14.6}\text{Al}_{10}$ MG,

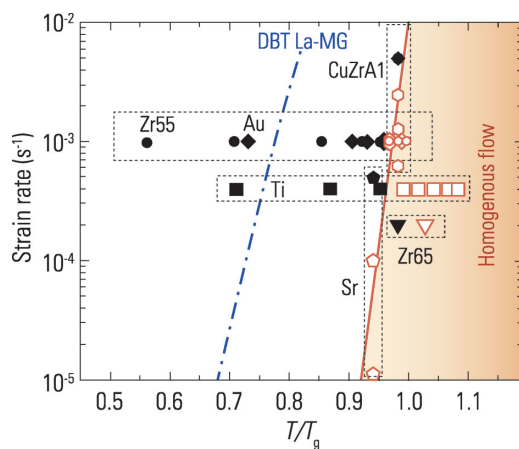


Figure 18. The deformation modes (brittle versus ductile) of six typical MGs compared with a La MG. They include $Zr_{55}Al_{10}Ni_5Cu_{30}$ ([158], circles), $Au_{49}Ag_{5.5}Pd_{2.3}Cu_{26.9}Si_{16.3}$ ([159], diamonds), $Cu_{46}Zr_{46}Al_8$ ([162], hexagons), $Ti_{40}Zr_{25}Ni_3Cu_{12}Be_{20}$ ([163], squares), $Zn_{20}Ca_{20}Sr_{20}Yb_{20}Li_{11}Mg_9$ ([164], pentagons), and $Zr_{65}Al_{7.5}Ni_{10}Cu_{17.5}$ ([165], triangles). The filled black symbols represent brittle fracture, while the open red symbols represent ductile deformation. The blue dashed curve is the brittle-to-ductile boundary of a $La_{68.5}Ni_{16}Al_{14}Co_{1.5}$ MG; to the right of this boundary the La MG shows significant tensile plasticity. In the shaded region, the MGs deform via homogeneous flow.

the crossover time is about $\tau_c = 277$ s at 540 K, determined from Fig. 20b. Fig. 20c shows the DMA curves (E'') of the same MG. Its β -relaxation manifests as a feeble relaxation hump or excess wing; the flank of a weak β -relaxation is submerged under a much stronger α -relaxation. This makes it hard to quantitatively determine the dynamics of the β -relaxation. Nevertheless, considering that the strengths E'' of β -relaxation in MGs are weakly temperature dependent and usually about 1/10 of that of the α -relaxation (see the section entitled ‘Low amplitude and increases with temperature’), it is plausible that β -relaxation occurs in the temperature and frequency regime marked in Fig. 20c. Plotting this regime together with the crossover time (converted to frequency via $\tau = 1/2\pi f$) in an Arrhenius frame, as shown in Fig. 20d, clearly indicates that both of them occur in the same temperature and time regime and even show similar Arrhenius dynamics. Further careful and well-considered experiments are expected to verify the above correlation. At even longer timescales or higher temperatures, another crossover associated with the α -relaxation can be expected.

Overall, the above findings from creep and stress relaxation demonstrate once again the intimate connections between β -relaxation and mechanical

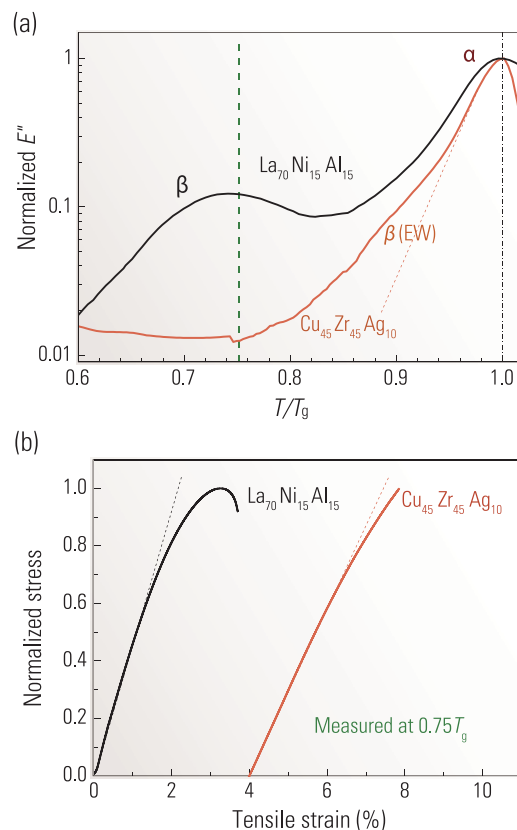


Figure 19. Comparative studies between a La MG and a CuZr MG (a) DMA spectra and (b) tensile stress–strain curves, redrawn from [167].

properties, and the importance of these connections in understanding the deformation mechanisms [11].

Shear band dynamics, activation of STZs, and the theoretical strength of MGs

At ambient and low temperature (strictly speaking, low scaled temperature, $T/T_g < 0.8$), plastic deformation of MGs is localized into shear bands [148], which concentrate large plastic strains in extremely thin ribbon-like regions. These shear localizations control the macroscopic ductility of MGs, and are thus of much current interest. There are substantial studies on various aspects of shear bands: their geometry, structures, initiation, propagation, temperature rises inside them, and structural softening as well as the evolution from STZs to shear bands.

In a wide range of mechanical deformation tests, including compression, bending, and indentation, shear bands manifest as serrated flow behavior in the stress–strain curves, i.e. the stress/strain drops and increases jerkily; a typical example is shown in Fig. 21a [177,178]. Although the serrated or intermittent plastic flow is widely observed, the underlying physical mechanism is still not well

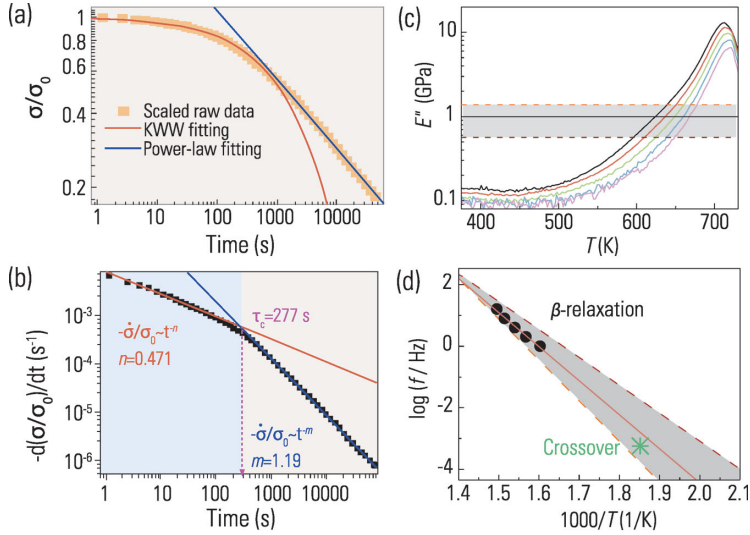


Figure 20. (a) Stress relaxation curve of a Zr MG, (b) derivative of (a) showing a crossover, (c) DMA spectrum of the Zr MG, and (d) comparison between the estimated β -relaxation time of the Zr MG and the crossover time in an Arrhenius frame. (a) and (b) are taken from [174] (Copyright 2013 American Institute Physics).

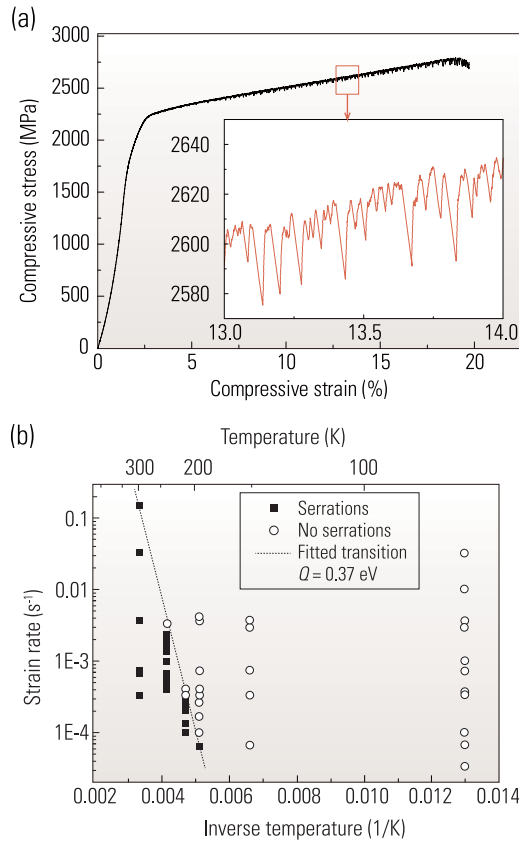


Figure 21. (a) A typical compressive deformation curve of a Zr MG; the inset shows serrated flow [177] (Copyright 2009 Acta Materialia Inc.). (b) Map of temperature and strain rate combinations for serrated flow, showing a boundary between serrated and non-serrated flow [179].

understood [178]. A characteristic feature of serrated flows is that they tend to be suppressed at high strain rates or low temperatures and disappear at some critical combinations of temperature and strain rate (as shown in Fig. 21b), which reflect a transition from serrated flow to non-serrated flow [179–182]. Some authors have found that this transition follows an Arrhenius relation in several MGs [179–182]. They found that the activation energies of these transitions, ΔE_s , range from 0.3 to 0.5 eV (30–50 kJ/mol) for typical Pd-, Zr-, and Fe-based MGs. Löffler and colleagues interpreted these values as being the activation energy associated with STZs [179]. However, it is noted that these values of ΔE_s are much smaller than those previously estimated using $W_{STZ} \approx E_\beta$. In Table 2, we collected the available data for ΔE_s , T_g , and the estimated $W_{STZ} \approx E_\beta \approx 26 RT_g$. One can see that the values of the ratio $\Delta E_s/W_{STZ}$ are nearly constant ~ 0.25 for all these MGs. This relationship implies that although ΔE_s may be related to W_{STZ} , they are not identical. We suggest that the small values of ΔE_s compared to W_{STZ} are caused by the fact that ΔE_s is measured at the yield stress, while the W_{STZ} values estimated from E_β are measured at very low stresses. In DMA measurements, the stress used is well below 10% of the yield stress.

We demonstrate here that such a difference between ΔE_s and W_{STZ} is consistent with the CSM and has implications for the understanding of the theoretical strength of MGs, another interesting topic. From the CSM, the height of the energy barrier to activation of an STZ, $W(\tau)$, decreases with increasing shear stress τ as

$$W_{STZ}(\tau) = 4RG_0\gamma_c^2 [(\tau_c - \tau)/\tau_c]^{3/2} \zeta \Omega N_0, \quad (8)$$

where τ_c is the stress at which $W_{STZ} = 0$, which is also the upper (ideal or theoretical) limit of strength of MGs from the CSM. Assuming that the volume of the STZ does not vary significantly with stress, one can obtain $W_{STZ}(\tau)/W_{STZ}(0) = (1 - \tau/\tau_c)^{3/2}$. Taking the experimental value $W_{STZ}(\tau_y)/W_{STZ}(0) = \Delta E_s/W_{STZ} = 0.25$, one can obtain $\tau_y/\tau_c \approx 0.6$ with τ_y the observed yield strength; this suggests that MGs yield macroscopically at 0.6 times their ideal stress. Recently, Tian *et al.* [184] performed *in situ* TEM tensile deformation of a $\text{Cu}_{50}\text{Zr}_{50}$ MG. By reducing the size of samples down to 100 nm to suppress shear banding, they found that the yield stress increased from the bulk value of 2.6 to 3.7 GPa, which approaches the ideal strength predicted above, because $2.6/0.6 \approx 4.3$ GPa. If in fact the volume of STZ increases at higher stress levels, the ideal strength of the $\text{Cu}_{50}\text{Zr}_{50}$ MG could be lower than 4.3 GPa and closer to the value found by

Table 2. Glass transition temperature T_g , activation energy of shear banding ΔE_s , and activation energy of the β -relaxation E_β [estimated from Equation (4)] for some typical MGs.

MG	T_g (K)	ΔE_s (kJ/mol)	E_β (kJ/mol)	$\Delta E_s/E_\beta$
Pd ₇₈ Cu ₆ Si ₁₆ [183, p. 213]	635	34	137	0.25
Ni ₇₀ Fe ₈ Si ₁₀ B ₁₂ [183, p. 213]	780	43	169	0.25
Co ₇₈ Si ₁₀ B ₁₂ [183, p. 213]	785	46	170	0.27
Vit105 [179]	663	31	143	0.22

Tian *et al.* Nevertheless, the above discussion provides a consistent scenario that unites the two seemingly different topics of shear-banding dynamics and the ideal strength of MGs from the perspectives of STZs and β -relaxations.

Shear banding has not yet been explored in detail from the perspective of β -relaxation, although its importance has been appreciated in the field of materials science [11,148]. We anticipate that this would be an emerging and fruitful research direction.

Similar correlations between β -relaxations and mechanical properties in polymer glasses

There are similar connections between β -relaxation and mechanical properties in polymer glasses [15–18,95–97,185–189]. Historically, after the birth of polymer materials in the 1920s and about two decades of research into the synthesis, characterization, and fabrication of plastics, researchers paid attention to the mechanical properties of these materials and tried to relate mechanical properties, such as impact strength, toughness, and creep resistance to molecular structures and dynamics. At first, one assumption frequently made was that all polymers, including rubbers, would be brittle at temperatures below T_g . But exceptions began to be recognized [15]. Then, researchers recognized that most polymers had transitions and relaxations lying below T_g , and that these secondary transitions appeared quite strong in polymers that were tough below their glass transition temperature. This gradually led to recognition of the importance of studying the relaxation spectra of polymers over a wide range of temperatures and frequencies as an aid in understanding their mechanical and physical behavior.

Heijboer [187–189] and Boyer [15], more or less simultaneously, proposed a relation between impact toughness and the damping peaks of β -relaxations that were observed in DMA or internal friction measurements. They suggested that polymers possessing low-temperature secondary transitions, especially those related to main-chain motions, would display good impact toughness at room temperature. As a

typical example, Fig. 22 compares the temperature-dependent yield stress of polycarbonate [15] and its $\tan(\delta)$ obtained from DMS [190]. The yield stress shows two distinct drops at the temperatures corresponding to the β - and α -relaxations, and this material becomes remarkably tough at room temperature after the full activation of the β -relaxation. There are a vast number of similar examples in polymers [15–18,95–97,185–189]; however, because of their complex chain structures and motions, there are also notable exceptions [15,191]. MGs, with very simple, atomic, structures, provide ideal model materials to examine this issue [11,35,43]. The similar connection between mechanical properties and β -relaxation in different glasses suggests that there must be some underlying universal physics yet to be discovered.

RELATIONSHIP BETWEEN RELAXATION AND DIFFUSION

MGs are also ideal materials for scientific study of fundamental issues in glassy physics. Over the past few years, diffusion in glasses and supercooled liquids has been a subject of considerable interest [3,12,117,192–195]. This is because diffusion is one of the most fundamental transport phenomena that occur in nature. For crystalline metals, diffusion (especially self-diffusion) occurs via single atomic jumps involving crystalline point defects, such as vacancies. However, the situation for glasses is much more complex. Early experiments were often interpreted in terms of a conventional vacancy-like mechanism. Now, there is substantial evidence that diffusion in the glassy state is highly collective, involving many atoms [192].

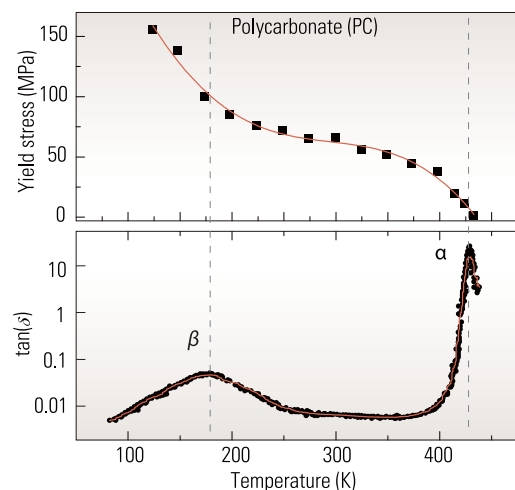


Figure 22. Comparison between (a) yield stress [15] and (b) $\tan(\delta)$ [190] of a polycarbonate.

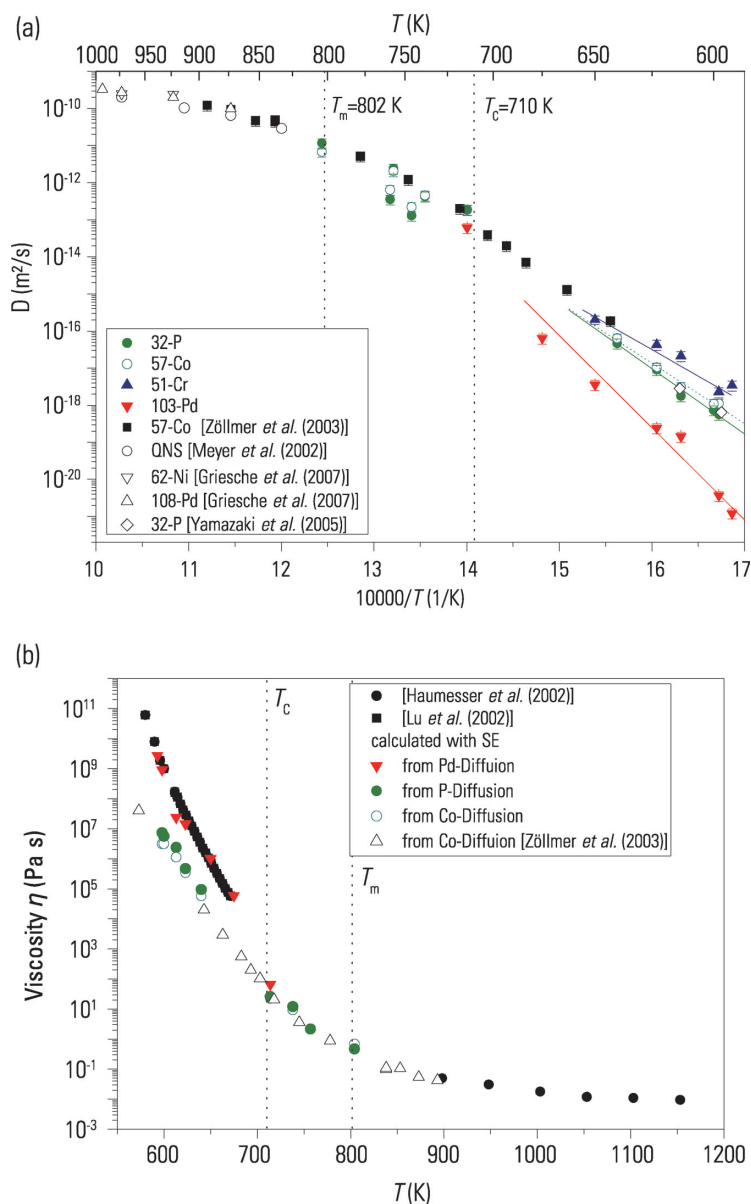


Figure 23. (a) Arrhenius plot for diffusion in liquid $\text{Pd}_{43}\text{Cu}_{27}\text{Ni}_{10}\text{P}_{20}$ alloys. (b) Comparison of diffusion and viscosity [202]. See [202] for the meanings of the labels (Copyright 2010 American Physics Society).

Besides the mechanism of diffusion itself, the relationship between diffusion and relaxations is an important topic that has been being actively discussed with regard to various glass-forming liquids [3,12]. At sufficiently high temperatures, α - and β -relaxations merge into a single relaxation, and the diffusion of different components becomes coupled. Relaxation and diffusion are usually connected by the Stokes–Einstein relation, which predicts that $D\eta/T$ or $D\tau_\alpha/T$ should be constants:

$$D = k_B T / (3\pi d \eta), \quad (9)$$

where D is the diffusion coefficient, d the effective particle radius, and η the viscosity; η and τ_α are connected by the Maxwell relationship:

$$\eta = G_\infty \tau_\alpha, \quad (10)$$

where G_∞ is the instantaneous shear modulus of the liquid. However, in many glass-forming liquids below approximately $1.2T_g$, there occurs a decoupling between D and η (or τ_α), as well as a decoupling of the diffusions of different components. In some fragile organic glasses near T_g , diffusive motions are faster than expected based on their τ_α (or η) by as much as six orders of magnitude. The origin of the breakdown of the Stokes–Einstein relation is an outstanding issue in glassy physics [77,186–201].

Diffusion decoupling and the Stokes–Einstein relation for the largest constituent atoms

Fig. 23a compares the diffusivities of Pd, Ni, Co, Cr, and P in a $\text{Pd}_{43}\text{Ni}_{10}\text{Cu}_{27}\text{P}_{20}$ melt, as collated by Bartsch *et al.* [202]. In an equilibrium melt (above melting temperature T_m) and down to the temperature range near T_c , all these probe atoms show similar diffusion behavior with nearly identical diffusivities, i.e. the diffusion of different components is coupled. However, at temperatures below T_c , significant decoupling of the component diffusivities can be observed and, importantly, atoms with smaller atomic size such as P and Cr have larger diffusivities compared with larger atoms, such as Pd (the largest atom in these glasses). This implies that atomic size disparity plays an important role in diffusion and this is directly related to the magnitude of diffusion decoupling: the smaller the atomic size, the faster the diffusion.

Fig. 23b shows viscosity data for a Pd-based MG former together with the diffusion data from Fig. 23a, converted into effective viscosity according to the Stokes–Einstein relation. It can be seen that the Stokes–Einstein relation, Equation (9), is well obeyed in normal liquids ($T > T_m$) for all the components, while disparities emerge at a temperature below T_c for different components. Remarkably, as found by Bartsch *et al.* [202], the Stokes–Einstein equation holds very well over at least 14 orders of magnitude for the slowest component Pd, which is also the majority component and has the largest atomic size. Other smaller atoms diffuse faster than the Pd atoms, and the Stokes–Einstein relation breaks down.

The above findings were explained by Bartsch *et al.* [202] from the perspective of atomic size

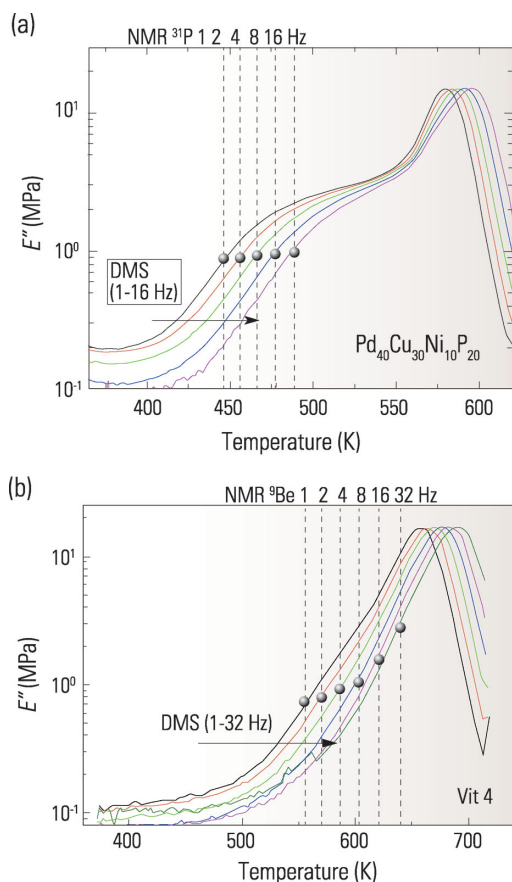


Figure 24. (a) Temperature dependence of E'' of $\text{Pd}_{40}\text{Ni}_{10}\text{Cu}_{30}\text{P}_{20}$ MG; the frequencies are 1, 2, 4, 8, and 16 Hz from left to right. The dashed lines are the NMR-probed P atom diffusive hopping rates (as indicated on the top) at the corresponding temperatures. (b) Same as (a) but for a Zr MG, where the dashed lines are the NMR-probed Be atom diffusive hopping rates. Adapted from [11,115] (Copyright 2013 American Physics Society).

disparity. Specifically, they suggested that Pd forms a slow subsystem in the supercooled melt, inside which the smaller elements carry out fast diffusion, while viscous flow requires rearrangement of the Pd subsystem.

Correlation between β -relaxation and diffusions of the smallest constituent atoms in MGs

The results of Bartsch *et al.* [202] led to another related question: what is the role of the smallest atoms in diffusion and relaxation? In a recent work [115], the dynamics of β -relaxations were compared with those of the self-diffusion of the smallest constituent atoms in MGs; these two processes were closely correlated.

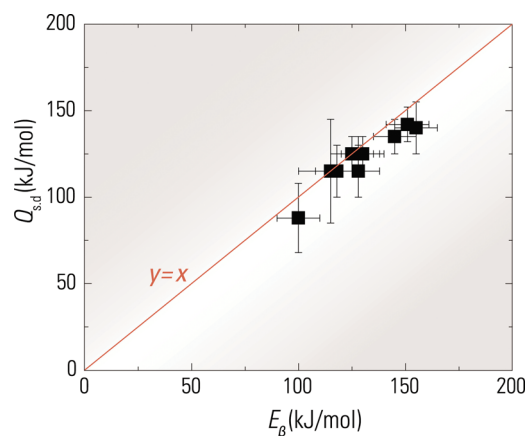


Figure 25. Comparison between the activation energy of β -relaxation E_β and the activation energy of self-diffusion of the smallest constituent atoms $Q_{s,d}$, in different MGs. A linear relation $y = x$ (the line) fits the data well [115] (Copyright 2013 American Physics Society).

Fig. 24a and b shows the E'' curves measured by DMA of two prototypical MGs, vit4 and $\text{Pd}_{40}\text{Ni}_{10}\text{Cu}_{30}\text{P}_{20}$, together with the temperature-dependent hopping frequencies of the smallest constituent atoms (Be in vit4 and P in $\text{Pd}_{40}\text{Ni}_{10}\text{Cu}_{30}\text{P}_{20}$) in the corresponding systems, as measured by NMR. An exciting observation is that the NMR data fall in the temperature and frequency range defined by the β -relaxations. As the hopping probed by is essentially a short-range form of diffusion, this finding suggests that the diffusion of the smallest atoms takes place at the same temperature and frequency range as the β -relaxation. Furthermore, as shown in Fig. 25, an equivalence between E_β and the activation energy for self-diffusion of the smallest constituent atoms $Q_{s,d}$ has been found to hold in many other MGs, irrespective of the techniques used to measure diffusion (e.g. NMR, tracer atoms, elastic back scattering) [115].

Mechanistically, as schematically shown in Fig. 26, Yu *et al.* [115] suggested the following scenario to explain the correlations between β -relaxation and self-diffusion of the smallest constituent atoms. As suggested by theoretical work and simulations, a β -event is considered to be a string of atoms that moves back and forth reversibly and cooperatively within the confinement provided by the surrounding elastic matrix. When two strings of atoms move towards each other and get close enough (as schematically shown by step 1 in Fig. 26b), the small atom at the end of one string could be attracted and taken over by the other string of atoms (step 2 in Fig. 26b), and then the two strings of atoms separate and move in opposite directions (step 3 in Fig. 26b). The net

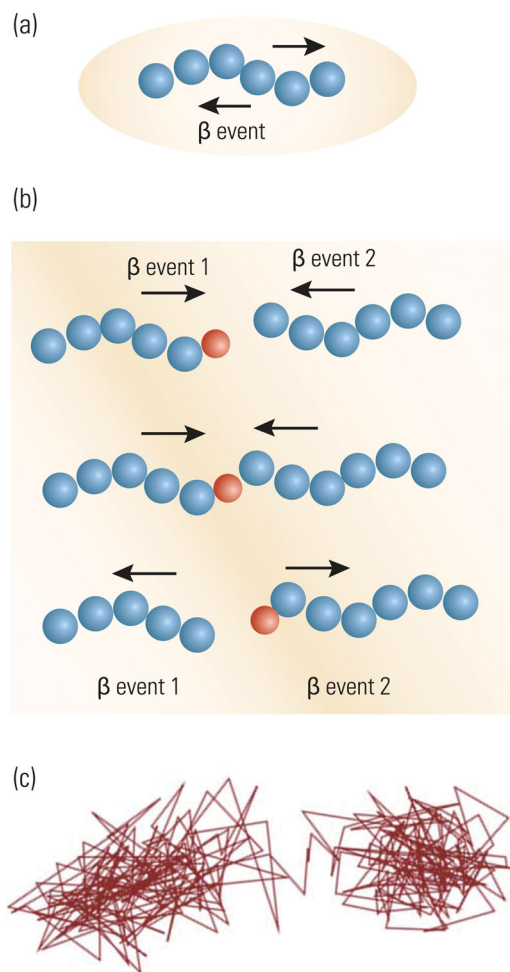


Figure 26. (a) Schematic diagram of atomic configurations and motions of a β -event in an MG. The ellipse represents the confinement of the elastic matrix. The two arrows represent the atoms moving back and forth reversibly. (b) Schematic diagram showing the relationship between β -events and diffusion. The smaller red circle indicates a diffusing atom. (c) The net motions corresponding to the smallest atoms in (b). (a) and (b) are adapted from [115] (Copyright 2013 American Physics Society).

result of this process is that the atom at the end of one string diffuses a small distance (Fig. 26c). As a consequence, the β -relaxations and diffusion of the smallest constituent atoms are intimately related; in effect, the smallest constituent atoms act as ‘tracers’ in probing β -relaxations in MGs. This picture suggests that the diffusion of the smallest constituent atoms is a consequence of several β -events. Certainly, Fig. 26 is only a 1 Dimensional cartoon for such a diffusion jump. In 3 D obviously there are other possibilities like a certain angle among the two strings.

The correlation between diffusion and β -relaxations in MGs is part of a controversial issue:

whether β -relaxation involves all the atoms or only a small fraction. Based on the above results, if all the smallest constituent atoms were to undergo diffusive-type motions associated with β -relaxation, the application of an external stress would induce viscous flow at the temperature and timescale of the β -relaxation, which has not been observed in any kind of glass so far. This implies that only a small fraction of the material takes part in the motions involved in β -relaxation of MGs.

Insights into the breakdown of the Stokes–Einstein relation

The results of Bartsch *et al.* [202] and Yu *et al.* [115] complement each other. Together, they suggest a connection between the decoupling of diffusion of different components and the splitting of the relaxation modes in MGs and MG-forming supercooled liquids. This also implies that β -relaxation could be responsible for the enhanced diffusivity and the breakdown of the Stokes–Einstein relation, as first suggested by Richert and Samwer [203].

In an MD simulation of hard sphere liquids, Kumar *et al.* [204] found that an appropriately defined slow subpopulation of particles (sedentary particles) follow the Stokes–Einstein relationship over a wide range of density, while the liquid as a whole violates this relationship. This observation provided evidence that some ‘hoppers’, which diffuse faster than average, are responsible for the breakdown of the Stokes–Einstein relationship. In connection to the above results in MGs, it can be inferred that the smallest atoms, promoted by β -relaxation, act as these hoppers, as shown in Fig. 26c.

These results [115,202,204] are also of interest within the general concept of dynamic asymmetry and its relation to size disparity. For instance, theoretical work and simulations have suggested that the glass transition (the arrest of the α -relaxation) is mainly controlled by slowing down of diffusion of large constituent particles, while diffusion of small particles persists deep into the glassy state [205–208]. Because of the large differences in sizes of their constituent atoms and relatively simple atomic structures, MGs and MG-forming liquids represent ideal systems to test these suggestions.

More recently, Ngai and Capaccioli [209] thought that the above results in MGs posed a big challenge to the traditional explanation of the breakdown of the Stokes–Einstein relation, which relied on dynamic heterogeneity arguments; instead, they provided fresh insights based on the coupling model, together with the correlation between β -relaxation and diffusion of the smallest atoms in the glassy system.

Diffusion in plastic deformed MGs and in shear bands

Since diffusion is extremely sensitive to local atomic environments, it provides a tool, although indirectly, to probe structural changes in plastically deformed MGs. Recently, Bokeloh *et al.* [210] performed measurements of Ag radiotracer diffusion in cold rolled Pd₄₀Ni₄₀P₂₀ MG. They found a surprisingly large enhancement of diffusion coefficient—about eight orders of magnitude higher than an undeformed sample (from the order of 10⁻¹⁷ to 10⁻²⁵ m²/s). Obviously, such a difference mainly arises from the presence of shear bands. Bokeloh *et al.* suggested that enhanced diffusion occurs via high-mobility pathways originating from some excess free volume distributed inside the shear bands. Although plausible, this qualitative suggestion does not allow a quantitative calculation of the enhancement. Recognizing the correlation between diffusion and β -relaxation, Ngai and Yu [211] recently demonstrated that such a result can be quantitatively rationalized within the framework of a coupling model. The underlying physics is that the interatomic cooperativity of the α -relaxation is drastically reduced for diffusion in shear bands, leading to much shorter relaxation times, which approach that of the β -relaxation [211].

Munch *et al.* [190] reported an interesting ‘plastic-deformation enhanced molecular mobility’ in a polycarbonate glass. They observed that plastic strain induced by mechanical rolling could change the DMS spectra in a unique way; a relaxation plateau appeared between the β - and α -relaxations, and the values of $\tan(\delta)$ were enhanced. It is still not clear whether phenomena similar to these (especially, the relaxation plateau) can occur in MGs [48].

Obviously, studying shear banding in MGs from the perspective of relaxation dynamics is an emerging and promising research direction.

CORRELATION BETWEEN β -RELAXATION AND STABILITY AND CRYSTALLIZATION OF MGs

Stability and crystallization are some of the major concerns in many applications of glassy materials [212–215]. Crystallization can drastically change many properties of glasses, including their mechanical, optical, electrical, and magnetic properties. In many cases, crystallization causes mechanical brittleness, loss of transparency, and decrease in electrical resistance. Crystallization also limits the processing of glasses, where stable viscous supercooled liquids are required [214]. On the other hand, crystal-

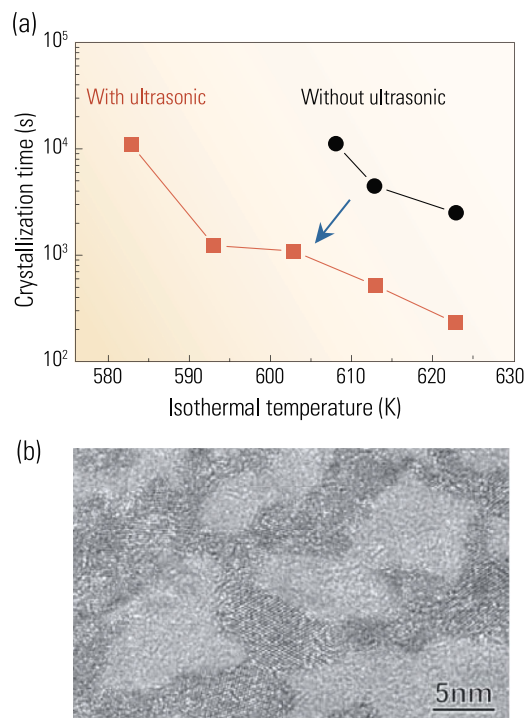


Figure 27. (a) Time–temperature–transformation diagram for Pd_{42.5}Ni_{7.5}Cu₃₀P₂₀ with or without ultrasonic perturbation, redrawn from the data of [221]. (b) Typical HRTEM image of the Pd MG after annealing at 290°C for 10 h under ultrasonic vibrations of 0.35 MHz [219] (Copyright 2005 American Physics Society).

lization of MGs has been used to produce nanocrystalline materials [216]. For some MGs, such as Al MG [217], crystallization can produce uniform nanocrystalline Al with face-centered cubic structures, having enhanced ductility [218].

Accelerated crystallization of MGs due to external fields

Crystallization of MGs usually occurs after the glass transition, i.e. $T_x > T_g$, where T_x is the temperature of the onset of crystallization. However, it was discovered that the perturbations from some external periodic fields can markedly accelerate crystallization and promote crystallization below T_g . The underlying mechanism is considered to be correlated with β -relaxations [219–221].

As a typical example, Fig. 27a reproduces the results of Ichitsubo *et al.* [221]. They constructed time–temperature–transformation diagrams for a Pd_{42.5}Ni_{7.5}Cu₃₀P₂₀ glass with and without ultrasonic perturbations. Clearly, under ultrasonic perturbations, the crystallization is greatly accelerated. Under ultrasonic vibrations of 0.35 MHz, the MG was found to be fully crystallized within only 18 h

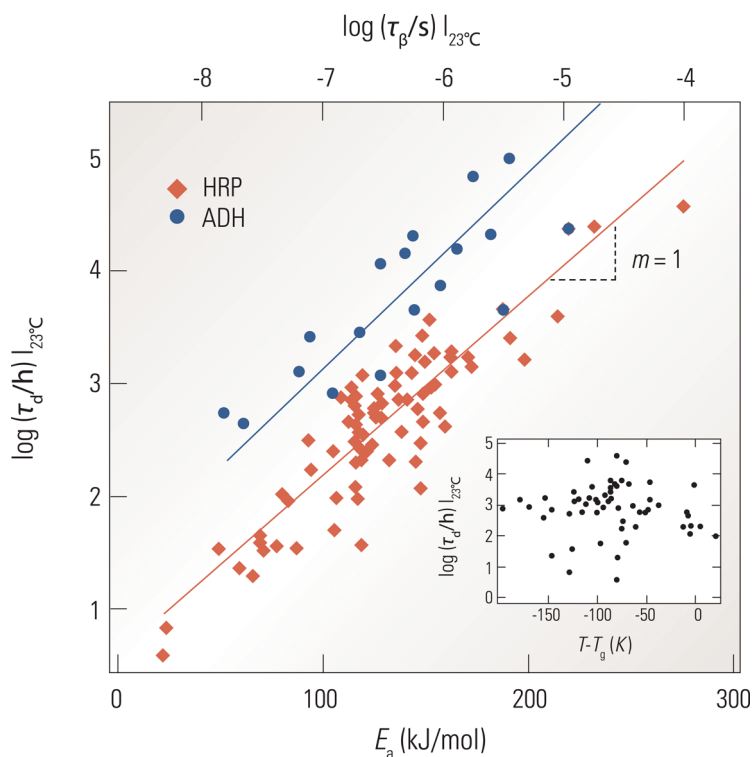


Figure 28. Comparison between β -relaxation time and the enzyme degradation rates at 23°C in hundreds of plasticized and antiplasticized sugar glasses. Adapted from [222].

at 290°C (10 K below T_g), while crystallization was negligible when the samples were annealed without ultrasonic vibrations for 75 h at the same temperature. They even obtained a semi-crystalline mixture mostly consisting of amorphous regions with a small amount of crystallized regions when the sample was ultrasonically annealed for 10 h. Fig. 27b [219] shows a corresponding HRTEM image. One can see that the amorphous regions are surrounded by crystallized walls that show lattice-fringe contrast. They also investigated the crystalline phases formed under ultrasonic perturbation and concluded that the ultrasonic annealing merely enhances the crystallization rate, but produces no particular phases [221]—demonstrating a purely dynamic effect.

Ichitsubo *et al.* [219–221] further estimated that at their annealing temperature the ultrasonic frequency was located within the β -relaxation range, and they proposed that the accelerated crystallization was caused by the accumulation of atomic jumps associated with β -relaxations being stochastically resonant with the ultrasonic vibrations. Besides, from the HRTEM, they proposed a microstructural model for fragile glasses, suggesting that MGs are intrinsically inhomogeneous, and contain both strongly bonded regions and weakly bonded regions. This model has been important to discussions of many properties of MGs.

The β -relaxation governs stability of glassy biomaterials

Cicerone and Douglas [222] presented convincing evidence that the stability of proteins in sugar-glass matrix materials, used to freeze-drying proteins and nucleic acids, is directly linked to the β -relaxation processes of the sugar matrix, instead of the commonly assumed α -relaxation. Specifically, they observed that when the β -relaxation time τ_β of sugar-glasses is increased with antiplasticizing additives, protein stability increases in linear proportion to the increase in τ_β , even though the same additives simultaneously decrease T_g and the α -relaxation time τ_α , of the sugar matrix material. Fig. 28 [222] shows degradation times τ_d , as a function of τ_β for two model proteins, horseradish peroxidase and equine alcohol dehydrogenase, at room temperature ($T = 23^\circ\text{C}$) for 22 antiplasticized sugar-glass systems, comprising more than 100 different glass formulations, as reported in [222]. The behavior of τ_d precisely mimics that of the β -relaxation. The degradation processes clearly track the β -relaxation, although the latter take places many orders of magnitude faster than the former.

Although the mechanism is not quite clear, these results suggest that, to enhance the stability of glassy materials, the activation of the β -relaxation must be retarded or suppressed. An example exploiting this idea has been given by Capaccioli *et al.* [5]. They found that the strong tendency of amorphous celecoxib (a powerful anti-inflammatory drug for treatment of arthritis) to crystallize can be reduced by mixing it with octa-acetylmaltose. Addition of only 10% of octa-acetylmaltose suppressed the β -relaxation in the glassy state and completely prevented devitrification of celecoxib [5].

The β -relaxation and ultrastable glasses

Recently, some novel amorphous materials, termed ‘ultrastable glasses (SGs)’, which exhibit remarkable thermodynamic and kinetic stabilities, have been prepared by vapor deposition routes together with appropriately high substrate temperatures [4,55,223–227]. These materials, besides their technological importance, are of special interest for understanding many fundamental issues regarding the nature of glass.

In considering the ability to form SGs, Yu *et al.* [55] demonstrated a modest correlation between liquid fragility and $\delta T_g/T_g$ (where δT_g is the enhancement in glass transition temperature T_g of the SG relative to that of the corresponding quenched glass), with a polymer glass, PMMA, at the highest extreme, and a Zr-based SMG approaching the

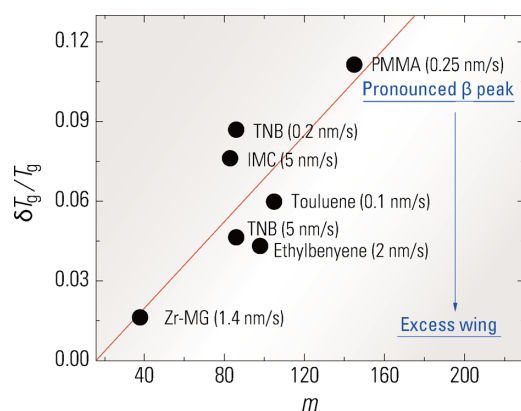


Figure 29. Correlation between fragility index m and $\delta T_g / T_g$ for different SGs; values in the parentheses are the deposition rates (Copyright 2013 Wiley-VCH Verlag GmbH & Co. KGaA, Weinheim) [55].

lowest extreme, as shown in Fig. 29. However, another factor relevant to the SG-forming ability, as first conceived by Chen and Richert [228], could be the occurrence or strength of a β -relaxation, which indicates that residual local mobility as a glass is formed. This suggestion is supported by the data shown in Fig. 29. For example, PMMA (with the largest value of $\delta T_g / T_g$) has a very pronounced β -relaxation (even stronger than its α -relaxation in dielectric and mechanical spectra), while the β -relaxation of the Zr-based SMG (which has the smallest value of $\delta T_g / T_g$) takes the form of excess wings. The underlying physical reason might be that at the combination of substrate temperature (about 0.8 – $0.95T_g$) and deposition rate (0.1 – 10 nm/s) used, surface dynamics are more controlled by β -relaxations. However, we note that the correlation is not conclusive, because δT_g is also dependent on other factors, such as deposition rates and substrate temperatures. Clarifying the mechanism of SG formation could be of great significance [55,223].

SUMMARY

This paper reviews the emerging field of β -relaxations in MGs, demonstrating their considerable potential to facilitate understanding of many critical unresolved issues in glassy physics and materials science—the glass transition, mechanical properties, shear-banding dynamics and deformation mechanisms, diffusion, breakdown of Stokes–Einstein relation, and crystallization and stability of glasses. These insights could provide the knowledge needed to design glassy materials with tunable properties (such as ductility and stability). However, at this stage, studies of β -relaxations in MGs are far from comprehensive. As well as the

specific aspects outlined in the text, some additional remarks can be made here.

- (i) There are a vast range of compositions of MGs with diverse physical and mechanical properties, and the β -relaxation behavior in these various MGs is far from fully explored. Since β -relaxations in MGs are sensitive to chemical effects, unexpected discoveries are likely to continue to occur when β -relaxations in more MGs are studied.
- (ii) Currently, the frequency ranges of DMA used to probe β -relaxations in MGs are quite limited (e.g. 10^{-2} to 10^2 Hz). Development of wider frequency DMA with high precision, and comparing results of such DMA with those obtained using other techniques (e.g. STM, NMR), would be highly valuable, with more intriguing results expected.
- (iii) Since the nature of β -relaxations is still unclear, computer simulations are urgently needed. There have been some recent attempts in this regard that may help understand the nature of the β -relaxation [140,229].
- (iv) Studying β -relaxations from the atomic and electronic structure perspectives are expected to give more fundamental insights. These could take the advantages of the relatively simple atomic structures of MGs [10,230].
- (v) It is foreseeable that β -relaxations in MGs could play increasingly important roles in understanding the nature of glasses and tailoring the properties of glassy materials for particular applications.

ACKNOWLEDGEMENTS

We thank Professor P. Lunkenheimer, Dr Jichao Qiao, Dr Zheng Wang, and Xuanqiao Gao for providing their original data and figures, as well as Professor Ranko Richert, Professor Kia L. Ngai, and Dr Robert Maaß for discussions/communications.

FUNDING

H.B. Yu acknowledges the Alexander von Humboldt Foundation (AvH) for post-doc support. W.H. Wang and H.Y. Bai acknowledge support from the National Natural Science Foundation of China (51271195). K. Samwer acknowledges support from the German Science Foundation (DFG).

REFERENCES

1. Dyre, J.C. Colloquium: the glass transition and elastic models of glass-forming liquids. *Rev Mod Phys* 2006; **78**: 953–72.
2. Lunkenheimer, P, Schneider, U and Brand, R *et al.* Glassy dynamics. *Contemp Phys* 2000; **41**: 15–36.

3. Angell, CA, Ngai, KL and McKenna, GB *et al.* Relaxation in glass forming liquids and amorphous solids. *J Appl Phys* 2000; **88**: 3113–57.
4. Ediger, MD and Harrowel, P. Perspective: supercooled liquids and glasses. *J Chem Phys* 2012; **137**: 080901.
5. Capaccioli, S, Paluch, M and Prevosto, D *et al.* Many-body nature of relaxation processes in glass-forming systems. *J Phys Chem Lett* 2012; **3**: 735–43.
6. Zachariasen, WH. The atomic arrangement in glass. *J Am Chem Soc* 1932; **54**: 3841–51.
7. Elliott, SR. Medium-range structural order in covalent amorphous solids. *Nature* 1991; **354**: 445–52.
8. Salmon, PS. Amorphous materials: order within disorder. *Nat Mater* 2002; **1**: 87–8.
9. Martin, JD, Goettler, SJ and Fosse, N *et al.* Designing intermediate-range order in amorphous materials. *Nature* 2002; **419**: 381–4.
10. Cheng, YQ and Ma, E. Atomic-level structure and structure-property relationship in metallic glasses. *Prog Mater Sci* 2011; **56**: 379–473.
11. Yu, HB, Wang, WH and Samwer, K. The β relaxation in metallic glasses: an overview. *Mater Today* 2013; **16**: 183–91.
12. Ngai, KL, *Relaxation and Diffusion in Complex Systems*. New York, NY: Springer, 2011.
13. Hu, LN, Yue, YZ and Bian, XF. A new threshold of uncovering the nature of glass transition: the slow β relaxation in glassy states. *Chin Sci Bull* 2010; **55**: 457–72.
14. Greer, AL. Metallic glasses... on the threshold. *Mater Today* 2009; **12**: 14–22.
15. Boyer, RF. Dependence of mechanical properties on molecular motion in polymers. *Polym Eng Sci* 1968; **8**: 161–85.
16. Engels, TAP, Govaert, LE and Meijer, HEH. Mechanical characterization of glassy polymers: quantitative prediction of their short- and long-term responses. In: Krzysztow, M and Martin, M (eds). *Polymer Science: A Comprehensive Reference*. Amsterdam: Elsevier, 2012, 723–47.
17. Retting, W. The relations between relaxation spectra, flaw growth, and ultimate properties of PVC. *Eur Polym J* 1970; **6**: 853–63.
18. Kalfoglou, NK and Williams, HL. Structure-property relationships of chlorinated polyethylenes. *Polym Eng Sci* 1972; **12**: 224–35.
19. Johari, GP and Goldstein, M. Viscous liquids and glass transition .2. Secondary relaxations in glasses of rigid molecules. *J Chem Phys* 1970; **53**: 2372–88.
20. Johari, GP and Goldstein, M. Viscous liquids and glass transition .3. Secondary relaxations in aliphatic alcohols and other nonrigid molecules. *J Chem Phys* 1971; **55**: 4245–52.
21. Johari, GP. Glass-transition and secondary relaxations in molecular liquids and crystals. *Ann NY Acad Sci* 1976; **279**: 117–40.
22. Johari, GP. Localized molecular motions of β relaxation and its energy landscape. *J Non-Cryst Solids* 2002; **307**: 317–25.
23. Ngai, KL and Paluch, M. Classification of secondary relaxation in glass-formers based on dynamic properties. *J Chem Phys* 2004; **120**: 857–73.
24. Klement, W, Willens, RH and Duwez, P. Non-crystalline structure in solidified gold-silicon alloys. *Nature* 1960; **187**: 869–70.
25. Wang, WH. Bulk metallic glasses with functional physical properties. *Adv Mater* 2009; **21**: 4524–44.
26. Ashby, MF and Greer, AL. Metallic glasses as structural materials. *Scripta Mater* 2006; **54**: 321–6.
27. Chen, HS and Morito, N. Sub-Tg α' relaxation in a PdCuSi glass; internal friction measurements. *J Non-Cryst Solids*, 1985; **72**: 287–99
28. Okumura, H, Chen, HS and Inoue, A *et al.* Structural relaxation of a La₅₅Al₂₅Ni₂₀ amorphous alloy measured by an internal friction method. *Jpn J Appl Phys* 1991; **30**: 2553.
29. Okumura, H, Chen, HS and Inoue, A *et al.* Sub-Tg mechanical relaxation of a La₅₅Al₂₅Ni₂₀ amorphous alloy. *J Non-Cryst Solids* 1991; **130**: 304–10.
30. Okumura, H, Chen, HS and Inoue, A *et al.* The observation of two glass transitions in the dynamic mechanical properties of a La₅₅Al₂₅Ni₂₀ amorphous alloy. *J Non-Cryst Solids* 1992; **150**: 401–5.
31. Peker, A and Johnson, WL. A highly processable metallic-glass—Zr_{41.2}Ti_{13.8}Cu_{12.5}Ni_{10.0}Be_{22.5}. *Appl Phys Lett* 1993; **63**: 2342–4.
32. Johnson, WL. Bulk glass-forming metallic alloys: science and technology. *MRS Bull* 1999; **24**: 42–56.
33. Inoue, A. Stabilization of metallic supercooled liquid and bulk amorphous alloys. *Acta Mater* 2000; **48**: 279–306.
34. Wang, WH, Dong, C and Shek, CH. Bulk metallic glasses. *Mater Sci Eng R* 2004; **44**: 45–89.
35. Yu, HB, Shen, X and Wang, Z *et al.* Tensile plasticity in metallic glasses with pronounced β relaxations. *Phys Rev Lett* 2012; **108**: 015504.
36. Pelletier, JM, Van de Moortèle, B and Lu, IR. Viscoelasticity and viscosity of Pd–Ni–Cu–P bulk metallic glasses. *Mater Sci Eng A* 2002; **336**: 190–5.
37. Wen, P, Zhao, DQ and Pan, MX *et al.* Relaxation of metallic Zr_{46.25}Ti_{18.25}Cu_{7.5}Ni₁₀Be_{27.5} bulk glass-forming supercooled liquid. *Appl Phys Lett* 2004; **84**: 2790.
38. Rosner, P, Samwer, K and Lunkenheimer, P. Indications for an ‘excess wing’ in metallic glasses from the mechanical loss modulus in Zr₆₅Al_{7.5}Cu_{27.5}. *Europhys Lett* 2004; **68**: 226–32.
39. Liu, XF, Zhang, B and Wen, P *et al.* The slow beta-relaxation observed in Ce-based bulk metallic glass-forming supercooled liquid. *J Non-Cryst Solids* 2006; **352**: 4013–6.
40. Zhao, ZF, Wen, P and Wang, WH *et al.* Observation of secondary relaxation in a fragile Pd₄₀Ni₁₀Cu₃₀P₂₀ bulk metallic glass. *Appl Phys Lett* 2006; **89**: 071920.
41. Wang, WH, Wen, P and Liu, XF. The excess wing of bulk metallic glass forming liquids. *J Non-Cryst Solids* 2006; **352**: 5103–9.
42. Zhao, ZF, Wen, P and Shek, CH *et al.* Measurements of slow β relaxations in metallic glasses and supercooled liquids. *Phys Rev B* 2007; **75**: 174201.
43. Yu, HB, Wang, WH and Bai, HY *et al.* Relating activation of shear transformation zones to β relaxations in metallic glasses. *Phys Rev B* 2010; **81**: 220201.
44. Yu, HB, Wang, Z and Wang, WH *et al.* Relation between beta relaxation and fragility in LaCe-based metallic glasses. *J Non-Cryst Solids* 2012; **358**: 869–71.
45. Wang, Z, Yu, HB and Wen, P *et al.* Pronounced slow β relaxation in La-based bulk metallic glasses. *J Phys-Condens Matter* 2011; **23**: 142202.
46. Qiao, JC and Pelletier, JM. Dynamic mechanical analysis in La-based bulk metallic glasses: secondary β and main α relaxations. *J Appl Phys* 2012; **112**: 083528.
47. Qiao, JC and Pelletier, JM. Mechanical relaxation in a Zr-based bulk metallic glass: analysis based on physical models. *J Appl Phys* 2012; **112**: 033518.
48. Qiao, JC, Pelletier, JM and Kou, HC *et al.* Modification of atomic mobility in a Ti-based bulk metallic glass by plastic deformation or thermal annealing. *Intermetallics* 2012; **28**: 128–37.
49. Liang, DD, Wang, XD and Ma, Y *et al.* Decoupling of pronounced β and α relaxations and related mechanical property change. *J Alloy Compd* 2013; **577**: 257–60.
50. Pineda, E, Bruna, P and Ruta, B *et al.* Relaxation of rapidly quenched metallic glasses: effect of the relaxation state on the slow low temperature dynamics. *Acta Mater* 2013; **61**: 3002–11.
51. Chen, HS. On mechanisms of structural relaxation in a Pd₄₈Ni₃₂P₂₀ glass. *J Non-Cryst Solids* 1981; **46**: 289–305.

52. Bershtein, VA and Egorov, VM. *Differential Scanning Calorimetry of Polymers*. New York, NY: Ellis Horwood, 1994.
53. Vyazovkin, S and Dranca, I. Probing beta relaxation in pharmaceutically relevant glasses by using DSC. *Pharm Res* 2006; **23**: 422–8.
54. Wang, T. *Ph.D. Dissertation*. Chinese Academy of Sciences Institute of Physics 2011.
55. Yu, HB, Luo, Y and Samwer, K. Ultrastable metallic glass. *Adv Mater* 2013; **25**: 5904–8.
56. Hornbøll, L and Yue, Y. Enthalpy relaxation of hyperquenched glasses and its possible link to α - and β -relaxations. *J Non-Cryst Solids* 2008; **354**: 350–4.
57. Hornbøll, L and Yue, Y. Enthalpy relaxation in hyperquenched glasses of different fragility. *J Non-Cryst Solids* 2008; **354**: 1862–70.
58. Hu, L and Yue, Y. Secondary relaxation behavior in a strong glass. *J Phys Chem B* 2008; **112**: 9053–7.
59. Hu, L and Yue, Y. Secondary relaxation in metallic glass formers: its correlation with the genuine Johari–Goldstein relaxation. *J Phys Chem C* 2009; **113**: 15001–6.
60. Hu, L, Zhou, C and Zhang, C *et al*. Thermodynamic anomaly of the sub-Tg relaxation in hyperquenched metallic glasses. *J Chem Phys* 2013; **138**: 174508.
61. Hu, L, Zhang, C and Yue, Y. Structural evolution during the sub-Tg relaxation of hyperquenched metallic glasses. *Appl Phys Lett* 2010; **96**: 221908.
62. Hu, L, Yue, Y and Zhang, C. Abnormal sub-Tg enthalpy relaxation in the CuZrAl metallic glasses far from equilibrium. *Appl Phys Lett* 2011; **98**: 081904.
63. Yue, YZ and Angell, CA. Clarifying the glass-transition behaviour of water by comparison with hyperquenched inorganic glasses. *Nature* 2004; **427**: 717–20.
64. Ashtekar, S, Scott, G and Lyding, J *et al*. Direct visualization of two-state dynamics on metallic glass surfaces well below Tg. *J Phys Chem Lett* 2010; **1**: 1941–5.
65. Ashtekar, S, Scott, G and Lyding, J *et al*. Direct imaging of two-state dynamics on the amorphous silicon surface. *Phys Rev Lett* 2011; **106**: 235501.
66. Kudlik, A, Tschirwitz, C and Blochowicz, T *et al*. Slow secondary relaxation in simple glass formers. *J Non-Cryst Solids* 1998; **235–237**: 406–11.
67. Deegan, RD and Nagel, SR. Dielectric susceptibility measurements of the primary and secondary relaxation in polybutadiene. *Phys Rev B* 1995; **52**: 5653–6.
68. Wagner, H and Richert, R. Equilibrium and non-equilibrium type β -relaxations: D-sorbitol versus o-terphenyl. *J Phys Chem B* 1999; **103**: 4071–7.
69. Richert, R, Duvvuri, K and Duong, LT. Dynamics of glass-forming liquids. VII. Dielectric relaxation of supercooled tris-naphthylbenzene, squalane, and decahydroisoquinoline. *J Chem Phys* 2003; **118**: 1828–36.
70. Jiao, W, Wen, P and Peng, HL *et al*. Evolution of structural and dynamic heterogeneities and activation energy distribution of deformation units in metallic glass. *Appl Phys Lett* 2013; **102**: 101903.
71. Paluch, M, Roland, CM and Pawlus, S *et al*. Does the Arrhenius temperature dependence of the Johari–Goldstein relaxation persist above Tg? *Phys Rev Lett* 2003; **91**: 115701.
72. Casalini, R, Snow, AW and Roland, CM. Temperature dependence of the Johari–Goldstein relaxation in poly(methyl methacrylate) and poly(thiomethyl methacrylate). *Macromolecules* 2012; **46**: 330–4.
73. Fujima, T, Frusawa, H and Ito, K. Merging of α and slow β relaxation in supercooled liquids. *Phys Rev E* 2002; **66**: 031503.
74. Martinez-Garcia, JC, Martinez-Garcia, J and Rzoska, SJ *et al*. The new insight into dynamic crossover in glass forming liquids from the apparent enthalpy analysis. *J Chem Phys* 2012; **137**: 064501–8.
75. Hedges, LO, Jack, RL and Garrahan, JP *et al*. Dynamic order-disorder in atomistic models of structural glass formers. *Science* 2009; **323**: 1309–13.
76. Mallamace, F, Branca, C and Corsaro, C *et al*. Transport properties of glass-forming liquids suggest that dynamic crossover temperature is as important as the glass transition temperature. *Proc Natl Acad Sci USA* 2010; **107**: 22457–62.
77. Casalini, R and Roland, CM. Viscosity at the dynamic crossover in o-terphenyl and salol under high pressure. *Phys Rev Lett* 2004; **92**: 245702.
78. Novikov, VN and Sokolov, AP. Universality of the dynamic crossover in glass-forming liquids: a ‘magic’ relaxation time. *Phys Rev E* 2003; **67**: 031507.
79. Mallamace, F, Branca, C and Corsaro, C *et al*. Dynamical crossover and breakdown of the Stokes–Einstein relation in confined water and in methanol-diluted bulk water. *J Phys Chem B* 2010; **114**: 1870–8.
80. Hachenberg, J, Bedorf, D and Samwer, K *et al*. Merging of the alpha and beta relaxations and aging via the Johari–Goldstein modes in rapidly quenched metallic glasses. *Appl Phys Lett* 2008; **92**: 131911.
81. Yu, HB, Samwer, K and Wang, WH *et al*. Chemical influence on β -relaxations and the formation of molecule-like metallic glasses. *Nat Commun* 2013; **4**: 2204.
82. Hodge, IM. Physical aging in polymer glasses. *Science* 1995; **267**: 1945–7.
83. Cangialosi, D, Boucher, VM and Alegría, A *et al*. Physical aging in polymers and polymer nanocomposites: recent results and open questions. *Soft Matter* 2013; **9**: 8619–30.
84. Lunkenheimer, P, Wehn, R and Schneider, U *et al*. Glassy aging dynamics. *Phys Rev Lett* 2005; **95**: 055702.
85. Johari, GP. Effect of annealing on the secondary relaxations in glasses. *J Chem Phys* 1982; **77**: 4619–26.
86. Schneider, U, Brand, R and Lunkenheimer, P *et al*. Excess wing in the dielectric loss of glass formers: a Johari–Goldstein β relaxation? *Phys Rev Lett* 2000; **84**: 5560–3.
87. Casalini, R and Roland, CM. Aging of the secondary relaxation to probe structural relaxation in the glassy state. *Phys Rev Lett* 2009; **102**: 035701.
88. Yardimci, H and Leheny, RL. Aging of the Johari–Goldstein relaxation in the glass-forming liquids sorbitol and xylitol. *J Chem Phys* 2006; **124**: 214503.
89. Wen, P, Zhao, ZF and Pan, MX *et al*. Mechanical relaxation in supercooled liquids of bulk metallic glasses. *Phys Status Solidi A* 2010; **207**: 2693–703.
90. Wang, Z. *Ph.D. Dissertation*. Chinese Academy of Sciences Institute of Physics 2012.
91. Qiao, J, Pelletier, JM and Casalini, R. Relaxation of bulk metallic glasses studied by mechanical spectroscopy. *J Phys Chem B* 2013; **117**: 13658–66.
92. Cangialosi, D, Boucher, VM and Alegría, A *et al*. Direct evidence of two equilibration mechanisms in glassy polymers. *Phys Rev Lett* 2013; **111**: 095701.
93. Mattsson, J, Bergman, R and Jacobsson, P *et al*. Chain-length-dependent relaxation scenarios in an oligomeric glass-forming system: from merged to well-separated α and β loss peaks. *Phys Rev Lett* 2003; **90**: 075702.
94. Leon, C, Ngai, KL and Roland, CM. Relationship between the primary and secondary dielectric relaxation processes in propylene glycol and its oligomers. *J Chem Phys* 1999; **110**: 11585–91.
95. Jho, JY and Yee, AF. Secondary relaxation motion in bisphenol-A polycarbonate. *Macromolecules* 1991; **24**: 1905–13.
96. Chen, LP, Yee, AF and Goetz, JM *et al*. Molecular structure effects on the secondary relaxation and impact strength of a series of polyester copolymer glasses. *Macromolecules* 1998; **31**: 5371–82.
97. Kanapitsas, A, Pissis, P and Karabanova, L *et al*. Broadband dielectric relaxation spectroscopy in interpenetrating polymer networks of polyurethane-copolymer of butyl methacrylate and dimethacrylate triethylene glycol. *Polym Gels Netw* 1998; **6**: 83–102.

98. Chen, LP, Yee, AF and Moskala, EJ. The molecular basis for the relationship between the secondary relaxation and mechanical properties of a series of polyester copolymer glasses. *Macromolecules* 1999; **32**: 5944–55.
99. Capaccioli, S and Ngai, KL. Relation between the alpha-relaxation and Johari–Goldstein beta-relaxation of a component in binary miscible mixtures of glass-formers. *J Phys Chem B* 2005; **109**: 9727–35.
100. Casalini, R and Roland, CM. Effect of crosslinking on the secondary relaxation in polyvinylethylene. *J Polym Sci B* 2010; **48**: 582–7.
101. Reiser, A, Kasper, G and Hunklinger, S. Effect of pressure on the secondary relaxation in a simple glass former. *Phys Rev Lett* 2004; **92**: 125701.
102. Kessairi, K, Capaccioli, S and Prevosto, D *et al.* Effect of temperature and pressure on the structural (alpha-) and the true Johari–Goldstein (beta-) relaxation in binary mixtures. *J Non-Cryst Solids* 2007; **353**: 4273–7.
103. Pronin, AA, Kondrin, MV and Lyapin, AG *et al.* Glassy dynamics under super-high pressure. *Phys Rev E* 2010; **81**: 041503.
104. Roland, CM, Hensel-Bielowka, S and Paluch, M *et al.* Supercooled dynamics of glass-forming liquids and polymers under hydrostatic pressure. *Rep Prog Phys* 2005; **68**: 1405–78.
105. Casalini, R and Roland, CM. Pressure evolution of the excess wing in a type-B glass former. *Phys Rev Lett* 2003; **91**: 015702.
106. Hensel-Bielowka, S, Paluch, M and Ngai, KL. Emergence of the genuine Johari–Goldstein secondary relaxation in m-fluoroaniline after suppression of hydrogen-bond-induced clusters by elevating temperature and pressure. *J Chem Phys* 2005; **123**: 014502.
107. Wang, WH. Correlation between relaxations and plastic deformation, and elastic model of flow in metallic glasses and glass-forming liquids. *J Appl Phys* 2011; **110**: 053521.
108. Williams, G and Watts, DC. Molecular motion in glassy state—effect of temperature and pressure on dielectric beta relaxation of polyvinyl chloride. *T Faraday Soc* 1971; **67**: 1971–99.
109. Williams, G. *Adv Polym Sci* 1979; **33**: 59.
110. Wagner, H and Richert, R. Spatial uniformity of the β -relaxation in D-sorbitol. *J Non-Cryst Solids* 1998; **242**: 19–24.
111. Vogel, M and Rössler, E. Slow beta process in simple organic glass formers studied by one- and two-dimensional ^2H nuclear magnetic resonance. I. *J Chem Phys* 2001; **114**: 5802–15.
112. Vogel, M and Rössler, E. Slow beta process in simple organic glass formers studied by one and two-dimensional ^2H nuclear magnetic resonance. II. Discussion of motional models. *J Chem Phys* 2001; **115**: 10883–91.
113. Döös, A, Paluch, M and Sillescu, H *et al.* From strong to fragile glass formers: secondary relaxation in polyalcohols. *Phys Rev Lett* 2002; **88**: 095701.
114. Vogel, M and Rössler, E. On the nature of slow β -process in simple glass formers: a ^2H NMR study. *J Phys Chem B* 2000; **104**: 4285–7.
115. Yu, HB, Samwer, K and Wu, Y *et al.* Correlation between β relaxation and self-diffusion of the smallest constituting atoms in metallic glasses. *Phys Rev Lett* 2012; **109**: 095508.
116. Sillescu, H. Heterogeneity at the glass transition: a review. *J Non-Cryst Solids* 1999; **243**: 81–108.
117. Ediger, MD. Spatially heterogeneous dynamics in supercooled liquids. *Ann Rev Phys Chem* 2000; **51**: 99–128.
118. Richert, R. Heterogeneous dynamics in liquids: fluctuations in space and time. *J Phys-Condens Matter* 2002; **14**: R703–38.
119. Jankowiak, R, Hayes, JM and Small, GJ. Spectral hole-burning spectroscopy in amorphous molecular-solids and proteins. *Chem Rev* 1993; **93**: 1471–502.
120. Schiener, B, Bohmer, R and Loidl, A *et al.* Nonresonant spectral hole burning in the slow dielectric response of supercooled liquids. *Science* 1996; **274**: 752–4.
121. Richert, R and Weinstein, S. Nonlinear dielectric response and thermodynamic heterogeneity in liquids. *Phys Rev Lett* 2006; **97**: 095703.
122. Bauer, T, Lunkenheimer, P and Kastner, S *et al.* Nonlinear dielectric response at the excess wing of glass-forming liquids. *Phys Rev Lett* 2013; **110**: 107603.
123. Huang, W and Richert, R. Dynamics of glass-forming liquids. XIII. Microwave heating in slow motion. *J Chem Phys* 2009; **130**: 194509.
124. Paluch, M, Wojnarowska, Z and Hensel-Bielowka, S. Heterogeneous dynamics of prototypical ionic glass KCN monitored by physical aging. *Phys Rev Lett* 2013; **110**: 015702.
125. Wojnarowska, Z, Roland, CM and Kolodziejczyk, K *et al.* Quantifying the structural dynamics of pharmaceuticals in the glassy state. *J Phys Chem Lett* 2012; **3**: 1238–41.
126. Micko, B, Tschirwitz, C and Rössler, EA. Secondary relaxation processes in binary glass formers: emergence of ‘islands of rigidity’. *J Chem Phys* 2013; **138**: 154501.
127. Brand, R, Lunkenheimer, P and Loidl, A. Relaxation dynamics in plastic crystals. *J Chem Phys* 2002; **116**: 10386–401.
128. Zuriaga, M, Pardo, LC and Lunkenheimer, P *et al.* New microscopic mechanism for secondary relaxation in glasses. *Phys Rev Lett* 2009; **103**: 075701.
129. Bedorf, D and Samwer, K. Length scale effects on relaxations in metallic glasses. *J Non-Cryst Solids* 2010; **356**: 340–3.
130. Schwabe, M, Kuechemann, S and Wagner, H *et al.* Activation volume of microscopic processes in amorphous $\text{Pd}_{77.5}\text{Cu}_{6.0}\text{Si}_{16.5}$ due to stress and temperature. *J Non-Cryst Solids* 2011; **357**: 490–3.
131. Stillinger, FH. A topographic view of supercooled liquids and glass formation. *Science* 1995; **267**: 1935–9.
132. Dyre, JC and Olsen, NB. Minimal model for beta relaxation in viscous liquids. *Phys Rev Lett* 2003; **91**: 155703.
133. Tanaka, H. Origin of the excess wing and slow β relaxation of glass formers: a unified picture of local orientational fluctuations. *Phys Rev E* 2004; **69**: 021502.
134. Saito, M, Kitao, S and Kobayashi, Y *et al.* Slow processes in supercooled o-terphenyl: relaxation and decoupling. *Phys Rev Lett* 2012; **109**: 115705.
135. Biroli, G and Bouchaud, JP. The random first-order transition theory of glasses: a critical assessment. In: Wolynes, PG and Lubchenko, V (eds). *Structural Glasses and Supercooled Liquids*. John Wiley & Sons, Inc., 2012, 31–113.
136. Stevenson, JD and Wolynes, PG. A universal origin for secondary relaxations in supercooled liquids and structural glasses. *Nat Phys* 2010; **6**: 62–8.
137. Johnson, WL and Samwer, K. A universal criterion for plastic yielding of metallic glasses with a $(T/T_g)^{2/3}$ temperature dependence. *Phys Rev Lett* 2005; **95**: 195501.
138. Harmon, JS, Demetriou, MD and Johnson, WL *et al.* Anelastic to plastic transition in metallic glass-forming liquids. *Phys Rev Lett* 2007; **99**: 135502.
139. Johnson, WL, Demetriou, MD and Harmon, JS *et al.* Rheology and ultrasonic properties of metallic glass-forming liquids: a potential energy landscape perspective. *MRS Bull* 2007; **32**: 644–50.
140. Cohen, Y, Karmakar, S and Procaccia, I *et al.* The nature of the β peak in the loss modulus of amorphous solids. *Europhys Lett* 2012; **100**: 36003.
141. Donati, C, Douglas, JF and Kob, W *et al.* Stringlike cooperative motion in a supercooled liquid. *Phys Rev Lett* 1998; **80**: 2338–41.
142. Schober, HR. Soft phonons in glasses. *Physica A* 1993; **201**: 14–24.

143. Ngai, KL, Wang, Z and Gao, XQ *et al.* A connection between the structural alpha-relaxation and the beta-relaxation found in bulk metallic glass-formers. *J Chem Phys* 2013; **139**: 014502.
144. Ngai, KL and Capaccioli, S. Relation between the activation energy of the Johari–Goldstein β relaxation and T_g of glass formers. *Phys Rev E* 2004; **69**: 031501.
145. Schuh, CA, Hufnagel, TC and Ramamurty, U. Mechanical behavior of amorphous alloys. *Acta Mater* 2007; **55**: 4067–109.
146. Wang, WH. The elastic properties, elastic models and elastic perspectives of metallic glasses. *Prog Mater Sci* 2012; **57**: 487–656.
147. Chen, MW. Mechanical behavior of metallic glasses: microscopic understanding of strength and ductility. *Ann Rev Mater Res* 2008; **38**: 445–69.
148. Greer, AL, Cheng, YQ and Ma, E. Shear bands in metallic glasses. *Mater Sci Eng R* 2013; **74**: 71–132.
149. Courtney, TH. *Mechanical Behavior of Materials*, McGraw-Hill Company, Inc., 2000.
150. Argon, AS. Plastic-deformation in metallic glasses. *Acta Metall* 1979; **27**: 47–58.
151. Falk, ML and Langer, JS. Dynamics of viscoplastic deformation in amorphous solids. *Phys Rev E* 1998; **57**: 7192–205.
152. Schall, P, Weitz, DA and Spaepen, F. Structural rearrangements that govern flow in colloidal glasses. *Science* 2007; **318**: 1895–9.
153. Zink, M, Samwer, K and Johnson, WL *et al.* Plastic deformation of metallic glasses: size of shear transformation zones from molecular dynamics simulations. *Phys Rev B* 2006; **73**: 172203.
154. Rodney, D and Schuh, C. Distribution of thermally activated plastic events in a flowing glass. *Phys Rev Lett* 2009; **102**: 235503.
155. Stevenson, JD and Wolynes, PG. On the surface of glasses. *J Chem Phys* 2008; **129**: 234514.
156. Madge, SV, Louzguine-Luzgin, DV and Lewandowski, JJ *et al.* Toughness, extrinsic effects and Poisson's ratio of bulk metallic glasses. *Acta Mater* 2012; **60**: 4800–9.
157. He, Q, Cheng, YQ and Ma, E *et al.* Locating bulk metallic glasses with high fracture toughness chemical effects and composition optimization. *Acta Mater* 2011; **59**: 202–15.
158. Pan, D, Inoue, A and Sakurai, T *et al.* Experimental characterization of shear transformation zones for plastic flow of bulk metallic glasses. *Proc Natl Acad Sci USA* 2008; **105**: 14769–72.
159. Liu, ST, Wang, Z and Peng, HL *et al.* The activation energy and volume of flow units of metallic glasses. *Scripta Mater* 2012; **67**: 9–12.
160. Kato, H, Ichitsubo, T and Igarashi, H *et al.* Correlation of dynamic and quasi-static relaxations: the cox-merz rule for metallic glass. *Appl Phys Lett* 2009; **95**: 231911.
161. Song, SX, Jang, JSC and Huang, JC *et al.* Inhomogeneous to homogeneous transition in an Au-based metallic glass and its deformation maps. *Intermetallics* 2010; **18**: 702–9.
162. Tian, YB, Lin, JG and Li, W *et al.* Deformation behavior of a Cu-based amorphous alloy under different strain rates. *J Appl Phys* 2011; **109**: 083508.
163. Huang, Y, Shen, J and Sun, Y *et al.* High temperature deformation behaviors of Ti₄₀Zr₂₅Ni₃Cu₁₂Be₂₀ bulk metallic glass. *J Alloy Compd* 2010; **504**: S82–5.
164. Zhao, K, Xia, XX and Bai, HY *et al.* Room temperature homogeneous flow in a bulk metallic glass with low glass transition temperature. *Appl Phys Lett* 2011; **98**: 141913.
165. Ge, Y, Song, W and Wang, X *et al.* Temperature and strain rate dependence of deformation behavior of Zr₆₅Al_{7.5}Ni₁₀Cu_{17.5}. *Mater Chem Phys* 2010; **124**: 25–8.
166. Zhang, B, Zhao, DQ and Pan, MX *et al.* Amorphous metallic plastic. *Phys Rev Lett* 2005; **94**: 205502.
167. Wang, Z, Wen, P and Huo, LS *et al.* Signature of viscous flow units in apparent elastic regime of metallic glasses. *Appl Phys Lett* 2012; **101**: 121906.
168. Gumbsch, P, Riedle, J and Hartmaier, A *et al.* Controlling factors for the brittle-to-ductile transition in tungsten single crystals. *Science* 1998; **282**: 1293–5.
169. Tanaka, M, Tarleton, E and Roberts, SG. The brittle–ductile transition in single-crystal iron. *Acta Mater* 2008; **56**: 5123–9.
170. Kursumovic, A and Cantor, B. Anelastic crossover and creep recovery spectra in Fe₄₀Ni₄₀B₂₀ metallic glass. *Scripta Mater* 1996; **34**: 1655–60.
171. Kursumovic, A, Scott, MG and Girt, E *et al.* Changes in the Young's modulus during structural relaxation of a metallic glass. *Scripta Metall* 1980; **14**: 1303–8.
172. Park, KW, Lee, CM and Wakeda, M *et al.* Elastostatically induced structural disordering in amorphous alloys. *Acta Mater* 2008; **56**: 5440–50.
173. Sandor, MT, Ke, HB and Wang, WH *et al.* Anelasticity-induced increase of the Al-centered local symmetry in the metallic glass La₅₀Ni₁₅Al₃₅. *J Phys-Condens Matter* 2013; **25**: 165701.
174. Jiao, W, Sun, BA and Wen, P *et al.* Crossover from stochastic activation to cooperative motions of shear transformation zones in metallic glasses. *Appl Phys Lett* 2013; **103**: 081904.
175. Schwabe, M, Bedorf, D and Samwer, K. Influence of stress and temperature on damping behavior of amorphous Pd_{77.5}Cu_{6.0}Si_{16.5} below T_g. *Eur Phys J E* 2011; **34**: 1–5.
176. Ke, HB, Wen, P and Peng, HL *et al.* Homogeneous deformation of metallic glass at room temperature reveals large dilatation. *Scripta Mater* 2011; **64**: 966–9.
177. Yu, HB, Hu, J and Xia, XX *et al.* Stress-induced structural inhomogeneity and plasticity of bulk metallic glasses. *Scripta Mater* 2009; **61**: 640–3.
178. Sun, BA, Yu, HB and Jiao, W *et al.* Plasticity of ductile metallic glasses: a self-organized critical state. *Phys Rev Lett* 2010; **105**: 035501.
179. Dubach, A, Dalla Torre, FH and Löffler, JF. Deformation kinetics in Zr-based bulk metallic glasses and its dependence on temperature and strain-rate sensitivity. *Phil Mag Lett* 2007; **87**: 695–704.
180. Dalla Torre, FH, Dubach, A and Schaeffli, J *et al.* Shear striations and deformation kinetics in highly deformed Zr-based bulk metallic glasses. *Acta Mater* 2008; **56**: 4635–46.
181. Maaß, R, Klaumünzer, D and Löffler, JF. Propagation dynamics of individual shear bands during inhomogeneous flow in a Zr-based bulk metallic glass. *Acta Mater* 2011; **59**: 3205–13.
182. Maaß, R, Klaumünzer, D and Villard, G *et al.* Shear-band arrest and stress overshoots during inhomogeneous flow in a metallic glass. *Appl Phys Lett* 2012; **100**: 071904.
183. Kimura, H and Masumoto, T. Strength, ductility and toughness—a study in model mechanics. In: Luborsky, FE (ed.). *Amorphous Metallic Alloys*, Butterworths, 1983.
184. Tian, L, Cheng, YQ and Shan, ZW *et al.* Approaching the ideal elastic limit of metallic glasses. *Nat Commun* 2012; **3**: 609.
185. Wu, S. Secondary relaxation, brittle–ductile transition temperature, and chain structure. *J Appl Polym Sci* 1992; **46**: 619–24.
186. Jafari, SH and Gupta, AK. Impact strength and dynamic mechanical properties correlation in elastomer-modified polypropylene. *J Appl Polym Sci* 2000; **78**: 962–71.
187. Heijboer, J. Modulus and damping of polymers in relation to their structure. *Brit Polym J* 1969; **1**: 3–14.

188. Heijboer, J. Secondary loss peaks in glassy amorphous polymers. *Int J Polym Mater Polym Biomater* 1977; **6**: 11–37.
189. Heijboer, J. Molecular origin of relaxations in polymers. *Ann NY Acad Sci* 1976; **279**: 104–16.
190. Munch, E, Pelletier, JM and Sixou, B *et al.* Characterization of the drastic increase in molecular mobility of a deformed amorphous polymer. *Phys Rev Lett* 2006; **97**: 207801.
191. Vincent, PI. Impact strength and mechanical losses in thermoplastics. *Polymer* 1974; **15**: 111–6.
192. Faupel, F, Frank, W and Macht, MP *et al.* Diffusion in metallic glasses and supercooled melts. *Rev Mod Phys* 2003; **75**: 237–80.
193. Tang, XP, Geyer, U and Busch, R *et al.* Diffusion mechanisms in metallic supercooled liquids and glasses. *Nature* 1999; **402**: 160–2.
194. Gaukel, C and Schober, HR. Diffusion mechanisms in under-cooled binary metal liquids of $Zr_{67}Cu_{33}$. *Solid State Commun* 1998; **107**: 1–5.
195. Boddeker, B and Teichler, H. Dynamics near free surfaces of molecular dynamics simulated $Ni_{0.5}Zr_{0.5}$ metallic glass films. *Phys Rev E* 1999; **59**: 1948–56.
196. Tarjus, G and Kivelson, D. Breakdown of the Stokes–Einstein relation in supercooled liquids. *J Chem Phys* 1995; **103**: 3071–3.
197. Geyer, U, Johnson, WL and Schneider, S *et al.* Small atom diffusion and breakdown of the Stokes–Einstein relation in the supercooled liquid state of the $Zr_{46.7}Ti_{8.3}Cu_{7.5}Ni_{10}Be_{27.5}$ alloy. *Appl Phys Lett* 1996; **69**: 2492–4.
198. Voronel, A, Veliyulin, E and Machavariani, VS *et al.* Fractional Stokes–Einstein law for ionic transport in liquids. *Phys Rev Lett* 1998; **80**: 2630–3.
199. Chen, SH, Mallamace, F and Mou, CY *et al.* The violation of the Stokes–Einstein relation in supercooled water. *Proc Natl Acad Sci USA* 2006; **103**: 12974–8.
200. Kumar, P, Buldyrev, SV and Becker, SR *et al.* Relation between the Widom line and the breakdown of the Stokes–Einstein relation in supercooled water. *Proc Natl Acad Sci USA* 2007; **104**: 9575–9.
201. Xu, L, Mallamace, F and Yan, Z *et al.* Appearance of a fractional Stokes–Einstein relation in water and a structural interpretation of its onset. *Nat Phys* 2009; **5**: 565–9.
202. Bartsch, A, Rätzke, K and Meyer, A *et al.* Dynamic arrest in multicomponent glass-forming alloys. *Phys Rev Lett* 2010; **104**: 195901.
203. Richert, R and Samwer, K. Enhanced diffusivity in supercooled liquids. *New J Phys* 2007; **9**: 36.
204. Kumar, SK, Szamel, G and Douglas, JF. Nature of the breakdown in the Stokes–Einstein relationship in a hard sphere fluid. *J Chem Phys* 2006; **124**: 214501.
205. Voigtmann, T and Horbach, J. Double transition scenario for anomalous diffusion in glass-forming mixtures. *Phys Rev Lett* 2009; **103**: 205901.
206. Bosse, J and Kaneko, Y. Self-diffusion in supercooled binary liquids. *Phys Rev Lett* 1995; **74**: 4023–6.
207. Kurita, R and Weeks, ER. Glass transition of two-dimensional binary soft-disk mixtures with large size ratios. *Phys Rev E* 2010; **82**: 041402.
208. Moreno, AJ and Colmenero, J. Anomalous dynamic arrest in a mixture of large and small particles. *Phys Rev E* 2006; **74**: 021409.
209. Ngai, KL and Capaccioli, S. An explanation of the differences in diffusivity of the components of the metallic glass $Pd_{43}Cu_{27}Ni_{10}P_{20}$. *J Chem Phys* 2013; **138**: 094504–5.
210. Bokeloh, J, Divinski, SV and Reglitz, G *et al.* Tracer measurements of atomic diffusion inside shear bands of a bulk metallic glass. *Phys Rev Lett* 2011; **107**: 235503.
211. Ngai, KL and Yu, HB. Origin of ultrafast Ag radiotracer diffusion in shear bands of deformed bulk metallic glass $Pd_{40}Ni_{40}P_{20}$. *J Appl Phys* 2013; **113**: 103508.
212. Clavaguera-Mora, MT, Clavaguera, N and Crespo, D *et al.* Crystallisation kinetics and microstructure development in metallic systems. *Prog Mater Sci* 2002; **47**: 559–619.
213. Perepezko, JH. Nucleation-controlled reactions and metastable structures. *Prog Mater Sci* 2004; **49**: 263–84.
214. Schroers, J. Processing of bulk metallic glass. *Adv Mater* 2010; **22**: 1566–97.
215. Yang, L, Miller, MK and Wang, XL *et al.* Nanoscale solute partitioning in bulk metallic glasses. *Adv Mater* 2009; **21**: 305–8.
216. Lu, K. Nanocrystalline metals crystallized from amorphous solids: nanocrystallization, structure, and properties. *Mater Sci Eng R* 1996; **16**: 161–221.
217. He, Y, Poon, SJ and Shiflet, GJ. Synthesis and properties of metallic glasses that contain aluminum. *Science* 1988; **241**: 1640–2.
218. Inoue, A. Amorphous, nanoquasicrystalline and nanocrystalline alloys in Al-based systems. *Prog Mater Sci* 1998; **43**: 365–520.
219. Ichitsubo, T, Matsubara, E and Yamamoto, T *et al.* Microstructure of fragile metallic glasses inferred from ultrasound-accelerated crystallization in Pd-based metallic glasses. *Phys Rev Lett* 2005; **95**: 245501.
220. Ichitsubo, T, Matsubara, E and Kai, S *et al.* Ultrasound-induced crystallization around the glass transition temperature for $Pd_{40}Ni_{40}P_{20}$ metallic glass. *Acta Mater* 2004; **52**: 423–9.
221. Ichitsubo, T, Matsubara, E and Chen, HS *et al.* Structural instability of metallic glasses under radio-frequency-ultrasonic perturbation and its correlation with glass-to-crystal transition of less-stable metallic glasses. *J Chem Phys* 2006; **125**: 154502.
222. Cicerone, MT and Douglas, JF. β -relaxation governs protein stability in sugar-glass matrices. *Soft Matter* 2012; **8**: 2983–91.
223. Swallen, SF, Kearns, KL and Mapes, MK *et al.* Organic glasses with exceptional thermodynamic and kinetic stability. *Science* 2007; **315**: 353–6.
224. Dawson, KJ, Kearns, KL and Yu, L *et al.* Physical vapor deposition as a route to hidden amorphous states. *Proc Natl Acad Sci USA* 2009; **106**: 15165–70.
225. Guo, Y, Morozov, A and Schneider, D *et al.* Ultrastable nanostructured polymer glasses. *Nat Mater* 2012; **11**: 337–43.
226. Singh, S, Ediger, MD and de Pablo, JJ. Ultrastable glasses from in silico vapour deposition. *Nat Mater* 2013; **12**: 139–44.
227. Aji, DPB, Hirata, A and Zhu, F *et al.* Ultrastrong and ultrastable metallic glass. 2013, arXiv:1306.1575.
228. Chen, Z and Richert, R. Dynamics of glass-forming liquids. XV. Dynamical features of molecular liquids that form ultra-stable glasses by vapor deposition. *J Chem Phys* 2011; **135**: 124515.
229. Fragiadakis, D and Roland, CM. Molecular dynamics simulation of the Johari–Goldstein relaxation in a molecular liquid. *Phys Rev E* 2012; **86**: 020501.
230. Yu, HB, Wang, WH and Bai, HY. An electronic structure perspective on glass-forming ability in metallic glasses. *Appl Phys Lett* 2010; **96**: 081902.